ErbB4 deletion in noradrenergic neurons in the locus coeruleus induces mania-like behavior via elevated catecholamines

Shu-Xia Cao[1,†], Ying Zhang[2,†], Xing-Yue Hu[1], Bin Hong[1], Peng Sun[2], Hai-Yang He[2], Hong-Yan Geng[2], Ai-Min Bao[2], Shu-Min Duan[2], Jian-Ming Yang[3], Tian-Ming Gao[3], Hong Lian[2,*], Xiao-Ming Li[1, 2,*]

[1]Affiliated Sir Run Run Shaw Hospital, Zhejiang University School of Medicine, Hangzhou, China; [2]Department of Neurobiology, Institute of Neuroscience, Key Laboratory of Medical Neurobiology of the Ministry of Health, Joint Institute for Genetics and Genome Medicine between Zhejiang University and University of Toronto, Collaborative Innovation Center for Brain Science, Zhejiang University School of Medicine, Hangzhou, China; [3]Department of Neurobiology, School of Basic Medical Sciences, Southern Medical University, Guangzhou, China

***For Correspondence**: lixm@zju.edu.cn (X-ML); honglian@zju.edu.cn (HL)

[†]These authors contributed equally to this work.

Competing interests: The authors declare that no competing interests exist.

Funding: See page 15

Impact statement: This study for the first time elaborate the important role of ErbB4 in noradrenergic neurons associated with mania pathogenesis.

Abstract Dysfunction of the noradrenergic (NE) neurons is implicated in the pathogenesis of manic-depressive psychosis (MDP). ErbB4 is highly expressed in NE neurons, and its genetic variation has been linked to MDP; however, how ErbB4 regulates NE neuronal function and contributes to MDP pathogenesis is unclear. Here we find that conditional deletion of ErbB4 in locus coeruleus (LC) NE neurons increases neuronal spontaneous firing through NMDA receptor hyperfunction, and elevates catecholamines in the cerebrospinal fluid (CSF). Furthermore, ErbB4-deficient mice present mania-like behaviors, including hyperactivity, reduced anxiety and depression, and increased sucrose preference. These behaviors are completely rescued by the anti-manic drug lithium or antagonists of catecholaminergic receptors. Our study demonstrates the critical role of ErbB4 signaling in regulating LC-NE neuronal function, reinforcing the view that dysfunction of the NE system may contribute to the pathogenesis of mania-associated disorder.

Introduction

Manic-depressive psychosis (MDP), diagnosed on the basis of manic episodes with or without depression, is a severely debilitating psychiatric disorder (Holden, 2008). Though risk genes and rodent models of MDP have been reported (Arey et al., 2013; Craddock and Sklar, 2009; Gouvea et al., 2016; Han et al., 2013; Roybal et al., 2007; Saul et al., 2012), the underlying pathogenic mechanism has not yet been clearly defined due to the phenotypic and genotypic complexity of this disorder (Harrison et al., 2017).

Several lines of evidence implicate the noradrenergic (NE) system in the pathology of MDP. For instance, the concentrations of norepinephrine and its metabolites are significantly upregulated in the cerebrospinal fluid (CSF) of MDP patients during the manic state (Kurita, 2016; Manji et al., 2003; Post et al., 1973; Post et al., 1978). In contrast, norepinephrine is downregulated in patients with depressive disorder (Maas et al., 1971; Moret and Briley, 2011; Wiste et al., 2008) and associated with mood transition in MDP patients (Kurita, 2016; Salvadore et al., 2010). However, how the NE system is involved in the pathology of MDP remains uncertain.

ErbB4, a receptor tyrosine kinase, plays a vital role in a number of biological processes, including neural development, excitability, and synaptic plasticity (Mei and Nave, 2014). In parvalbumin-positive (PV) interneurons, ErbB4 is involved in the etiology of schizophrenia and epilepsy (Chen et al., 2010; Del Pino et al., 2013; Fisahn et al., 2009; Li et al., 2012; Tan et al., 2012). ErbB4 mRNA is also prominently expressed in locus coeruleus (LC) NE neurons (Gerecke, 2001), and coding variants of *ERBB4* are genetically associated with MDP susceptibility (Chen et al., 2012; Goes et al., 2011). However, how ErbB4 regulates NE neuronal function and whether NE neuron-specific ErbB4 signaling participates in the pathogenesis of MDP is unknown.

In this study, we achieved ErbB4 deletion primarily in NE neurons by crossing *TH-Cre* mice (Gelman et al., 2003), in which Cre recombinase is mainly expressed in NE neurons of the LC (see Figure 1A-E and Discussion section), with mice carrying the loxP-flanked *Erbb4* allele ($Erbb4^{loxP/loxP}$). ErbB4 deletion increases the spontaneous firing of LC-NE neurons in an NMDA receptor-dependent manner, and elevates the concentrations of norepinephrine and dopamine in the CSF. Furthermore, $TH\text{-}Cre;Erbb4^{loxP/loxP}$ mice manifest a mania-like behavioral profile that can be recapitulated by $Erbb4^{loxP/loxP}$ mice with region-specific ablation of ErbB4 in the LC. In addition, treatment with lithium, a commonly used clinical anti-manic drug, or antagonists against dopamine or norepinephrine receptors all rescue the mania-like behaviors in $TH\text{-}Cre;Erbb4^{loxP/loxP}$ mice. Taken together, our study linked ErbB4 physiological function with NE system homeostasis and demonstrated the pathogenic effect of ErbB4 dysregulation in NE neurons in mania-associated psychiatric diseases.

Results

ErbB4 is primarily deleted from LC-NE neurons in *TH-Cre;Erbb4*$^{loxP/loxP}$ mice

To determine Cre distribution in our specific *TH-Cre* mouse line, we crossed *TH-Cre* mice with Ai9 mice to label Cre-positive neurons with red fluorescent protein tdTomato (Madisen et al., 2010). We examined Cre expression in the LC, ventral tegmental nucleus (VTA), and substantia nigra pars compacta (SNC) of Ai9;*TH-Cre* mice at postnatal day (P) 50 because tyrosine hydroxylase (TH), the key enzyme for the synthesis of norepinephrine and dopamine, is mainly expressed in these three areas. Colocalization analysis of TH staining and tdTomato suggested that in the rostral part of the LC, approximately 40% of TH-positive (TH+) neurons were Cre/Tomato-positive (Cre/Tomato+) and 92% of Cre/Tomato+ neurons were TH+, whereas in the caudal part of the LC, Cre/Tomato+ neurons only constituted 14% of TH+ neurons, with 82% of Cre/Tomato+ neurons being TH+ (Figure 1A, B). The VTA and SNC contain approximately 70% of the dopaminergic neurons in the brain (Bjorklund and Dunnett, 2007). Unexpectedly, in contrast to the LC, there were very few Cre/Tomato+ neurons in the VTA and SNC. Cre/Tomato was only expressed in approximately 1.6% and 0.9% of neurons in the rostral and caudal VTA, respectively. Moreover, only 2.1% of neurons in the rostral and caudal parts of the SNC were Cre/Tomato+. In the rostral and caudal parts of the VTA and SNC, only 8% and 12% of Cre/Tomato+ neurons, respectively, were TH+ (Figure 1A, B). To exclude possible false-positive signals introduced by the reporter mouse line, we took advantage of Ai3 mice, another reporter mouse strain that labels Cre-positive neurons with green fluorescent protein (GFP), to confirm these results. Consistently, we observed very little Cre expression in the VTA or SNC (Figure 1-figure supplement 1). These data suggest that Cre recombinase was primarily expressed in the NE neurons of the LC in our *TH-Cre* mouse line.

To investigate its role in NE neurons, we deleted ErbB4 in NE neurons by crossing *TH-Cre* with *Erbb4*$^{loxP/loxP}$ mice (Figure 1C). Immunoblotting analysis showed that ErbB4 was significantly decreased in the LC of *TH-Cre;Erbb4*$^{loxP/loxP}$ mice (Figures 1D, E, and Figure 1-figure supplement 2) with no significant change in the midbrain (VTA and SNC) (Figure 1D, E), which is consistent with our previous observation that Cre was mainly expressed in LC-NE neurons in *TH-Cre* mice. Immunohistochemical analysis also confirmed the deletion of ErbB4 in the LC (Figure 1F). In addition, we observed no obvious changes in cell density or soma size of LC neurons in *TH-Cre;Erbb4*$^{loxP/loxP}$ mice compared to control mice (Figures 1F and Figure 1-figure supplement 3).

Hyperactive LC-NE neurons in *TH-Cre;Erbb4*$^{loxp/loxp}$ mice increase extracellular norepinephrine and dopamine

To analyze the influence of ErbB4 deficiency on LC-NE neuronal physiology, we measured the spontaneous activity of LC-NE neurons in *TH-Cre;Erbb4*$^{loxp/loxp}$ mice in cell-attached configuration. Consistent with previous studies, LC-NE neurons recorded from slices of the control mice exhibited a firing rate of 2 ± 0.26 Hz (Chandler et al., 2014; Jedema and Grace, 2004) (Figure 2A, C). However, the spontaneous firing rate of LC-NE neurons in the *TH-Cre;Erbb4*$^{loxp/loxp}$ mice was significantly increased (3.04 ± 0.29 Hz) (Figure 2B, C), and the interspike interval was significantly decreased (Figure 2D).

Previous studies have demonstrated that neuronal excitability can affect the expression and phosphorylation of TH, the rate limiting factor in catecholamine synthesis (Aumann et al., 2011; Chevalier et al., 2008; Lew et al., 1999; Zigmond et al., 1989). Using protein extracts of LC tissues from controls and mutants, we measured the expression of phosphorylated TH (TH-Ser40), an active form of TH required for norepinephrine synthesis, along with other enzymes involved in norepinephrine homeostasis, including dopamine beta-hydroxylase (DBH), norepinephrine transporter (NET), and catechol-O-methyltransferase (COMT). We observed a marked increase in TH-Ser40 but not in total TH (Figures 2E, F, and Figure 2-figure supplement 1). In contrast, DBH, another enzyme involved in norepinephrine synthesis, and NET and COMT, which regulate norepinephrine degradation, were unchanged (Figure 2E, F). Thus, changes in the neuronal excitability of LC-NE neurons in *TH-Cre;Erbb4*$^{loxp/loxp}$ mice may specifically increase TH phosphorylation. Using lysates from the midbrain, none of these proteins showed any changes (Figure 2G, H), suggesting region-specific norepinephrine synthetic activity influenced in mutant animals.

As LC-NE neurons are the major source of norepinephrine in the forebrain (Sara, 2009), we hypothesized that the increase in NE neuronal and TH activities in the LC might increase the level of norepinephrine in the brain. Therefore, we examined the norepinephrine level in *TH-Cre;Erbb4*$^{loxp/loxp}$ mice using *in vivo* microdialysis in the lateral ventricle of anaesthetized mice, followed by high-performance liquid chromatography (HPLC). Results showed that norepinephrine concentration was significantly increased in the CSF of *TH-Cre;Erbb4*$^{loxp/loxp}$ mice (Figures 2I and Figure 2-figure supplement 2). Given that dopamine, the precursor of norepinephrine, is coupled with changes in norepinephrine level and can be co-released with norepinephrine by NE neurons (Devoto et al., 2005; Guiard et al., 2008; Pozzi et al., 1994; Yamamoto and Novotney, 1998), we also examined the concentration of dopamine in the CSF in *TH-Cre;Erbb4*$^{loxp/loxp}$ mice. Remarkably, the concentration of dopamine was also obviously increased compared with that in the control mice (Figures 2J and Figure 2-figure supplement 2).

Taken together, the increased excitability of LC-NE neurons may increase TH phosphorylation, resulting in the increase of norepinephrine and dopamine observed in the CSF of *TH-Cre;Erbb4*$^{loxp/loxp}$ mice.

Increased spontaneous firing of LC-NE neurons in *TH-Cre;Erbb4$^{loxp/loxp}$* mice due to NMDA receptor hyperfunction

An increase in glutamatergic synaptic input (Jodo and Aston-Jones, 1997; Somogyi and Llewellyn-Smith, 2001), or decrease in feedback inhibition from α-2-adrenoceptor, an autoreceptor (Langer, 1980; Starke, 2001), may contribute to the increased firing rate of LC-NE neurons. Moreover, in studies on the hippocampus and prefrontal cortex, the NMDA receptor, especially its subunit isoform NR2B, is reported to be regulated by ErbB4 (Hahn et al., 2006; Pitcher et al., 2011). Therefore, we examined the expression of NR2B and autoreceptors α-2A (A2A) and α-2C (A2C) using protein samples from the LC. Results showed that the expression of NR2B was significantly increased in *TH-Cre;Erbb4$^{loxp/loxp}$* mice, whereas no changes were detected in the expressions of NR1, A2A, or A2C (Figure 3A, B).

We hypothesized that the increase in NE neuronal activity might be attributed to strengthened NMDA receptor function correlated with NR2B overexpression in *TH-Cre;Erbb4$^{loxp/loxp}$* mice. Using the patch clamp technique, we found that the spontaneous firing rates and interspike intervals of LC-NE neurons in *TH-Cre;Erbb4$^{loxp/loxp}$* mice were rescued by the NMDA receptor antagonist APV (50 μM) (Figure 3C, D, and E). Thus, NMDA receptors appear to mediate the hyperexcitability of LC-NE neurons in *TH-Cre;Erbb4$^{loxp/loxp}$* mice.

TH-Cre;Erbb4$^{loxP/loxP}$ mice show mania-like behaviors

The LC is involved in mood, reward, and motor ability (Borodovitsyna et al., 2017; Dickinson et al., 1988; Neophytou et al., 2001). As ErbB4 was mainly deleted from the LC-NE neurons in *TH-Cre;Erbb4$^{loxP/loxP}$* mice, we hypothesized that *TH-Cre;Erbb4$^{loxP/loxP}$* mice might exhibit LC-related behavioral abnormalities. We first examined the motor ability of *TH-Cre;Erbb4$^{loxP/loxP}$* mice using the open field test. *TH-Cre;Erbb4$^{loxP/loxP}$* mice traveled longer distances and at higher speeds than control mice (Figure 4A-E) and spent less time immobile (Figure 4F). To examine anxiety- and depression-related behaviors of *TH-Cre;Erbb4$^{loxP/loxP}$* mice, we conducted the elevated plus maze test (EPM) and forced swim test. In the EPM, *TH-Cre;Erbb4$^{loxP/loxP}$* mice spent more time in and presented more entries into the open arms compared with the control mice (Figure 4G-I). In the forced swim test, *TH-Cre;Erbb4$^{loxP/loxP}$* mice showed less immobility (Figure 4J) and longer latency to first surrender compared with the control mice (Figure 4K). To examine the responses of *TH-Cre;Erbb4$^{loxP/loxP}$* mice to a natural reward, we performed the sucrose preference test. During this test, *TH-Cre;Erbb4$^{loxP/loxP}$* mice displayed increased preference for sucrose compared with the control mice (Figure 4L). No significant deficits in body weight or prepulse inhibition were observed in *TH-Cre;Erbb4$^{loxP/loxP}$* mice (Figure 4-figure supplement 1). These data indicate that *TH-Cre;Erbb4$^{loxP/loxP}$* mice exhibited hyperactivity, decreased anxiety and depression, and increased sucrose preference, thus resembling the phenotypes of rodent mania models (Arey et al., 2013;

Cosgrove et al., 2015; Han et al., 2013; Kirshenbaum et al., 2011; Nestler and Hyman, 2010; Prickaerts et al., 2006; Roybal et al., 2007; Shaltiel et al., 2008).

Region-specific deletion of ErbB4 in the LC causes mania-like behaviors

To exclude the possibility that the *TH-Cre;Erbb4*$^{loxP/loxP}$ mouse phenotypes were attributed to Cre-expressing neurons in other brain areas, we tested whether region-specific deletion of ErbB4 in the LC was sufficient to induce mania-like behaviors. We injected an adeno-associated virus (AAV) expressing Cre and GFP (AAV-Cre-GFP) into the LC of *Erbb4*$^{loxP/loxP}$ mice bilaterally. Cre/GFP was expressed abundantly in the LC (Figure 5A), with 52% of LC neurons being Cre/GFP-positive (Cre/GFP+) and 77.7% of Cre/GFP+ neurons being TH+ (Figure 5-figure supplement 1). Immunoblotting confirmed the efficiency of the ErbB4 deletion, showing significantly decreased ErbB4 in the LC of *Erbb4*$^{loxP/loxP}$ mice after AAV-Cre-GFP injection (Figure 5B). Behavioral tests were carried out 4 weeks after viral injection. In the open field test, viral-mediated region-specific deletion of ErbB4 in the LC significantly increased locomotor activity and traveling speed (Figure 5C, D), and both the distance and time traveled at high speed were significantly increased (Figure 5E, F). Moreover, the immobility time in the open area was significantly reduced (Figure 5G). In the EPM, ErbB4 deletion in the LC significantly increased both the time in and number of entries into the open arms (Figure 5H, I). In the forced swim test, mice with LC ErbB4 deletion exhibited decreased immobility time and increased latency to first surrender (Figure 5J, K). In the sucrose preference test, LC ErbB4 deletion significantly increased sucrose preference of the injected mice (Figure 5L). These results indicate that region-specific deletion of ErbB4 in the LC was sufficient to induce similar mania-like behaviors as those manifested in *TH-Cre;Erbb4*$^{loxP/loxP}$ mice.

Lithium treatment in *TH-Cre;Erbb4*$^{loxp/loxp}$ mice rescues behavioral, molecular, and electrophysiological abnormalities

Lithium was the first medicine approved by the Food and Drug Administration for MDP treatment. Testing the effect of lithium treatment on the behavioral abnormalities of *TH-Cre;Erbb4*$^{loxp/loxp}$ mice may validate those behaviors to be mania-like and also reveal whether NE neurons are involved in the mechanism of lithium.

After mice were treated for 10 d with lithium chloride (600 mg L^{-1}) dissolved in drinking water, as described previously (Roybal et al., 2007), the behavioral performance of *TH-Cre;Erbb4*$^{loxp/loxp}$ mice was rescued in the open field test, EPM, forced swim test, and sucrose preference test (Figure 6). In the open field test, lithium decreased locomotor activity, traveling speed, and distance and time traveled at high speed, and increased immobility time of *TH-Cre;Erbb4*$^{loxp/loxp}$ mice (Figure 6A-E). In addition, lithium decreased both time in and entries into the open arms by *TH-Cre;Erbb4*$^{loxp/loxp}$ mice in the EPM (Figure 6F-G). The treated *TH-Cre;Erbb4*$^{loxp/loxp}$ mice also exhibited significantly

increased immobility time and decreased latency to first surrender in the forced swim test (Figure 6H, I), and reduced sucrose preference in the sucrose preference test (Figure 6J).

To better understand the mechanisms underlying the effect of lithium on mania-like behaviors of *TH-Cre;Erbb4*$^{loxp/loxp}$ mice, Western blotting and patch clamp recordings were performed to detect TH phosphorylation and spontaneous firing of LC-NE neurons after lithium treatment, respectively. The phosphorylation of TH was significantly decreased in *TH-Cre;Erbb4*$^{loxp/loxp}$ mice receiving lithium (Figure 6K, L), whereas no change was observed in the protein levels of TH or the membrane-bound and soluble forms of COMT (MB-COMT and S-COMT, respectively) (Figure 6K, L). In addition, the spontaneous firing rates and interspike intervals of LC-NE neurons in *TH-Cre;Erbb4*$^{loxp/loxp}$ mice were both rescued after lithium treatment (Figure 6M, N).

These results indicate that NE neurons may be a potential target of lithium in the treatment of mania. In addition, the rescuing effect of lithium on the behavioral abnormalities of *TH-Cre;Erbb4*$^{loxp/loxp}$ mice further indicated that the behaviors induced by ErbB4 deletion in LC-NE neurons are mostly mania-like phenotypes.

Increase in norepinephrine and dopamine contributes to mania-like behaviors in *TH-Cre;Erbb4*$^{loxp/loxp}$ mice

Our previous results showed that both norepinephrine and dopamine were increased in *TH-Cre;Erbb4*$^{loxp/loxp}$ mice (Figure 2I, J). To identify which system contributes to the mania-like behaviors of *TH-Cre;Erbb4*$^{loxp/loxp}$ mice, norepinephrine α1 receptor antagonist prazosin (1 mg/kg, i.p.) and dopamine D1 receptor antagonist SCH23390 (0.125 mg/kg, i.p.) were used to inhibit the effects of norepinephrine and dopamine, respectively. Both prazosin and SCH23390 decreased the locomotor activity and traveling speed of *TH-Cre;Erbb4*$^{loxp/loxp}$ mice in the open field test (Figure 7A, B). Furthermore, both distance and time traveled at high speed decreased (Figure 7C, D), and the immobility time was markedly increased (Figure 7E) after prazosin and SCH23390 treatment. In the EPM test, prazosin and SCH23390 treatment in *TH-Cre;Erbb4*$^{loxp/loxp}$ mice decreased the time spent in the open arms, although no effect on the number of entries was observed (Figure 7F, G). Moreover, *TH-Cre;Erbb4*$^{loxp/loxp}$ mice treated with prazosin or SCH23390 exhibited increased immobility time and decreased latency to first surrender in the forced swim test (Figure 7H, I). In the sucrose preference test, prazosin and SCH23390 both significantly decreased the sucrose preference of *TH-Cre;Erbb4*$^{loxp/loxp}$ mice (Figure 7J). Taken together, these results demonstrate that increases in norepinephrine and dopamine contribute to the mania-like behaviors of *TH-Cre;Erbb4*$^{loxp/loxp}$ mice.

Discussion

We show that disruption of ErbB4 in LC-NE neurons causes NMDA receptor-mediated hyperactive spontaneous firing of LC-NE neurons and elevates CSF norepinephrine and dopamine concentrations, which induce mania-like behaviors that could be rescued by lithium or noradrenergic and dopaminergic receptor antagonists. This is the first study to demonstrate the function of ErbB4 in the regulation of behavior and mood by LC-NE neurons and of catecholamine dyshomeostasis in the pathogenesis of mania-associated disorders such as MDP.

MDP is a severe psychiatric disorder with a long-term global disease burden; however, its pathogenic mechanisms remain unknown (Harrison et al., 2017). Despite the increase of norepinephrine in MDP patient brains in mania episodes observed since early in the twentieth century (Manji et al., 2003; Post et al., 1973; Post et al., 1978), a clear description of a causal role played by norepinephrine in the pathophysiology of MDP is lacking. Here, for the first time, we demonstrates direct causality between catecholamine dyshomeostasis and mania behavior, as well as the important role of ErbB4 in MDP pathogenesis. Conditional ErbB4 deletion in LC-NE neurons increased the concentration of both norepinephrine and dopamine in the CSF, which is consistent with clinical observations of MDP patients. By specifically blocking the function of norepinephrine or dopamine, we restored the mania-like behaviors of *TH-Cre;Erbb4*$^{loxp/loxp}$ mice, providing strong evidence that elevated norepinephrine directly contributes to MDP pathogenesis. These findings will facilitate a better understanding of the pathophysiology of diseases associated with mania beyond MDP. The increased dopamine level may be attributable to the co-release of dopamine in NE neurons and the regulation of dopamine by NE neuronal terminals (Carboni et al., 1990; Devoto et al., 2005; Pozzi et al., 1994; Yamamoto and Novotney, 1998).

The mechanism underlying lithium treatment for MDP is complicated and unresolved (Jope, 1999; Schloesser et al., 2012). Here we showed that lithium rescued the abnormal spontaneous firing activity and TH phosphorylation of LC-NE neurons and alleviated mania-like behaviors in *TH-Cre;Erbb4*$^{loxp/loxp}$ mice (Figure 6). These observations suggest that LC-NE neurons may be a target of lithium and thus provide a possible mechanism for lithium treatment of MDP. In contrast to the manifestation in mutant mice, lithium treatment led to increased movement and decreased immobile time in the forced swim test in control mice (Figure 6), suggesting different functions of lithium in physiological and pathological statuses.

The LC is a nucleus consisting of most of the NE neurons in the brain, and its impairment has been implicated in many severe neurodegenerative diseases and affective disorders (Benarroch, 2009; Berridge and Waterhouse, 2003; Gary Aston-Jones 2005; Mather and Harley, 2016; Pamphlett, 2014; Ross et al., 2015). Though norepinephrine has been linked with MDP, direct evidence of how the LC functions in the pathogenesis of MDP is still unclear (Bernard et al., 2011; Bielau et al., 2012; Kato, 2008). Here, we provide direct evidence demonstrating the crucial role of the LC in MDP pathogenesis.

Erbb4 is a genetic susceptibility gene for schizophrenia (Mei and Xiong, 2008; Pitcher et al., 2011), with many studies reporting the crucial role of ErbB4 in the pathogenesis of schizophrenia (Chong et al., 2008; Del Pino et al., 2013; Hahn et al., 2006; Shamir et al., 2012). While coding variants of *Erbb4* have also been genetically associated with MDP (Chen et al., 2012; Goes et al., 2011), direct evidence remains limited. We reveal that functional deficiency of ErbB4 in LC-NE neurons facilitates the paroxysm of mania-like behaviors and increases spontaneous firing of LC-NE neurons (Figure 2A-D). In contrast, conditional ErbB4 deletion in parvalbumin-positive GABAergic neurons in the frontal cortex decreases the excitability of these neurons via $KV_{1.1}$ (Li et al., 2012). These lines of evidence suggest that ErbB4 may function differently in different neurons.

The NMDA receptor, especially its subunit isoform NR2B, is regulated by ErbB4 in the hippocampus and prefrontal cortex (Bjarnadottir et al., 2007; Pitcher et al., 2011). Consistent with previous studies on the influence of ErbB4 on NR2B, we observed NR2B overexpression in LC tissue of ErbB4-deficient mice (Figure 3A-B). However, how ErbB4 deletion increases NR2B protein expression and how NR2B overexpression participates in the strengthening of NMDA receptor function in the hyperexcitability of ErbB4-deficient NE neurons requires further investigation.

Past studies have reported ErbB4 mRNA to be highly expressed in the LC area (Gerecke, 2001). We confirmed ErbB4 protein expression in LC-NE neurons (Figure 1F). In addition, we functionally validated the presence of ErbB4 in LC-NE neurons by showing increased spontaneous firing and TH phosphorylation upon ErbB4 deletion. However, a previous report failed to detect the expression of Cre/Tomato in LC neurons in *ErbB4::CreERT2;Rosa::LSL-tdTomato* mice (Bean et al., 2014). This discrepancy may arise from the different experimental methods adopted by the different research groups.

Earlier research has shown that Cre is abundantly expressed in *TH-Cre* mouse lines in the NE and dopaminergic neurons of the LC and midbrain, respectively (Lindeberg et al., 2004; Savitt et al., 2005). Recent research used the *TH-Cre* line (Gong et al., 2007) to drive ErbB4 selective deletion, with gene loss mainly observed in dopaminergic neurons in the midbrain (Gong et al., 2007; Skirzewski et al., 2017). In contrast, very low Cre expression was detected in the midbrain dopaminergic neurons in our *TH*-Cre mice (Gelman et al., 2003) compared with the abundant Cre expression observed in the LC-NE neurons. Though mice of the same genotype (both *TH-Cre;Erbb4*$^{loxp/loxp}$) were used, the varied Cre expression in the distinct *TH-Cre* lines in our research and that of Skirzewski et al. (2017) yielded different findings on ErbB4 function in different neuronal types. ErbB4 deletion in dopaminergic neurons in the midbrain led to deficits in spatial/working memory but had no influence on locomotion or anxiety (Skirzewski et al., 2017). In comparison, our mutant mice with ErbB4 deletion in LC-NE neurons presented significant hyperactivity and reduced anxiety (Figure 4). The reason underlying the discrepancy between different *TH-Cre* lines is currently unknown (Lammel et al., 2015). One

probable explanation may be that *Cre* is inserted into different chromosomal loci and the surrounding genetic or epigenetic elements may modify the spatial and temporal regulation of *Cre* gene expression.

Together, our findings demonstrate the importance of ErbB4 in LC-NE neurons in behavior and mood regulation and reveal the participation of catecholamine homeostasis modulated by ErbB4 in the pathogenesis of mania-associated disorders. Future studies aimed at identifying ErbB4 downstream signals in LC-NE neurons may provide new insights into therapies for mania-associated disorders.

Materials and methods

Generation and maintenance of mice

Two mouse lines were used. We first crossed *TH-Cre* mice (kindly provided by Yuqiang Ding, Tongji University School of Medicine, Shanghai, China), which have been described previously (Gelman et al., 2003), with *Erbb4*$^{loxP/loxP}$ mice (Mutant Mouse Regional Resource Center from North America), generating a *TH-Cre;Erbb4*$^{loxp/loxp}$ mouse line in which ErbB4 was mainly deleted in the noradrenergic neurons (NE neurons). For electrophysiological recordings, we then crossed *TH-Cre;Erbb4*$^{loxp/loxp}$ mice with Ai9 mice, which are used as a Cre reporter strain (purchased from Jackson Laboratory). Only male mice (8–12 weeks old) with normal appearance and weight were used in experiments and were divided into different groups randomly. All mice were housed under a 12-h light/dark cycle and had access to food and water *ad libitum*.

Immunohistochemical analysis

Mice were anesthetized with 10% chloral hydrate and perfused with ice-cold saline followed by paraformaldehyde (PFA) (4%) in phosphate-buffered saline (PBS). Brains were removed and fixed in the same 4% PFA solution at 4°C overnight and transferred to 30% sucrose in PBS for 2 d. Frozen brains were sectioned at 30 μm with a sliding microtome (Leica CM3050 S, Leica biosystems) in the coronal plane. Slices were immersed in PBS with 0.02% sodium azide and stored at 4°C until further use. After incubation in blocking buffer containing 5% goat serum and 3% bovine serum albumin (BSA) in PBST (0.5% Triton X-100 in PBS) for 1 h at room temperature, slices were incubated with primary antibodies (rabbit tyrosine hydroxylase (TH)-specific antibody (1:700, Abcam), mouse ErbB4-specific antibody (1:300, Abcam)) in blocking buffer at 4°C overnight. The slices were washed three times in PBST and incubated with Alexa Fluor 488- or Alexa Fluor 543-conjugated secondary antibodies at 25°C for 1 h. All slices were counterstained with DAPI during final incubation. Fluorescent image acquisition was performed with an Olympus FluoView FV1000 confocal microscope using a 20× objective lens and analyzed using ImageJ software.

Western blot analysis.

Brain tissues were homogenized in RIPA lysis buffer containing 50 mM Tris (pH 7.4), 150 mM NaCl, 1% Triton X-100, 1% sodium deoxycholate, 0.1% SDS, 1 mM PMSF, and phosphatase inhibitor cocktail (Cell Signaling Technology). Protein samples were loaded on 10% acrylamide SDS-PAGE gels and then transferred to nitrocellulose membranes. After incubation with 4% BSA for 1 h at 25°C, membranes were incubated with primary antibodies at 4°C overnight

294 (sheep TH-specific antibody, 1:2,000, Millipore; rabbit TH-Ser40-specific antibody, 1:1,000, Millipore; rabbit ErbB4-
295 specific antibody, 1:2,000, Abcam; rabbit norepinephrine transporter (NET)-specific antibody, 1:300, Millipore; rabbit
296 dopamine beta-hydroxylase (DBH)-specific antibody, 1:300, Abcam; rabbit GAPDH-specific antibody, 1:5,000, Cell
297 Signaling Technology; mouse catechol-o-methyltransferase (COMT)-specific antibody, 1:5,000, BD Biosciences; and
298 rabbit actin-specific antibody, 1:2,000, Cell Signaling Technology). The membranes were washed three times and then
299 incubated for 1 h with horseradish peroxidase-conjugated secondary antibodies in 4% BSA at 25°C. Immunoreactive
300 bands were visualized clearly by X-ray film exposure (ECL kit, Thermo Scientific) and analyzed using NIH ImageJ
301 software. Each experiment was repeated at least three times.

302 ## Surgery and microdialysis

303 Mice were deeply anesthetized with isoflurane (0.15% in oxygen gas) and mounted on a stereotaxic frame (RWD Life
304 Science). A stainless steel guide cannula with a dummy probe was implanted into the lateral ventricle (anteroposterior
305 (AP) = −0.6 mm; mediolateral (ML) = ±1.2 mm; dorsoventral (DV) = −2.0 mm). After 7 d of recovery, the dummy probe
306 was replaced with a microdialysis probe (membrane length: 4 mm, molecular weight cut-off: 18,000 Da, outer diameter:
307 0.2 mm). For balance, artificial cerebrospinal fluid (ACSF), which contained (in mM) 125 NaCl, 2.5 KCl, 2 $CaCl_2$, 1
308 $MgCl_2$, 1.25 NaH_2PO_4, 25 $NaHCO_3$, and 11 D-glucose, was perfused continuously by syringe pump at a speed of 2 µl
309 min^{-1} for 2 h before sample collection. Samples (60 µl each) were automatically collected from each mouse for 2 h and
310 analyzed by high-performance liquid chromatography (HPLC) with an electrochemical detector (5014b, ESA, USA). The
311 concentrations of norepinephrine and dopamine were detected by HPLC (Coulochem III, ESA, USA) using a C18
312 column (MD150 3 mm × 150 mm, 5 µm, ESA, USA).

313 ## Slice preparation

314 Mice were deeply anesthetized and decapitated. The brain was quickly removed and immersed in ice-cold high-sucrose
315 ACSF bubbled with 95% O_2/5% CO_2 to maintain a pH of 7.4. High-sucrose ACSF contained the following (in mM): 200
316 sucrose, 3 KCl, 2 $CaCl_2$, 2 $MgCl_2$, 1.25 NaH_2PO_4, 26 $NaHCO_3$, and 10 D-glucose. Coronal slices (250 µm) were
317 prepared with a vibratome (Leica, VT 1000S, Germany), allowed to rest for 1 h at 34°C in oxygenated ACSF, and then
318 maintained at 25°C before transfer to the recording chamber.

319 ## Electrophysiology

320 Acute slices from adult mice were transferred to a recording chamber and fully submerged in ACSF at 25°C, which was
321 continuously perfused (2 ml/min) with oxygen. Fluorescent neurons were visually identified under an upright microscope

(Nikon, Eclipse FN1) equipped with an infrared-sensitive CCD camera with a ×40 water-immersion lens (Nikon, ECLIPSE FN1), and extracellular recordings were performed in cell-attached mode (MultiClamp 700B Amplifier, Digidata 1440A analog-to-digital converter). Microelectrodes (3–5 MΩ) were filled with a solution containing 130 mM potassium gluconate, 20 mM KCl, 10 mM HEPES buffer, 2 mM MgCl·6 H_2O, 4 mM Mg-ATP, 0.3 mM Na-GTP, and 10 mM EGTA; the pH was adjusted to 7.25 with 10 M KOH. Following a 3-min stabilization period, spontaneous firing was recorded for at least 4 min for each neuron. All analyses were performed using Clampfit 10.2 (Axon Instruments/Molecular Devices).

Virus vectors and stereotactic injection

AAV-GFP and AAV-hSyn-Cre-GFP were purchased from Shanghai SBO Medical Biotechnology Company, Shanghai. For viral injection, 1-month-old *Erbb4*$^{loxP/loxP}$ mice were anesthetized with chloral hydrate (400 mg/kg of body weight) by intraperitoneal (i.p.) injection and placed in a stereotactic frame, with their skulls then exposed by scalpel incision. Glass microelectrodes were used to bilaterally inject 0.15 µl of purified and concentrated AAV (~ 10^{11} infections units per ml) into the locus coeruleus (LC) (coordinates from bregma: anterior-posterior, 5.25 mm; lateral-medial, 1.00 mm; dorsal-ventral, –4.5 mm) at 100 nl min^{-1}. The injection microelectrode was slowly withdrawn 2 min after virus infusion.

Behavioral assays

All experiments were performed between 13:00 and 16:00. The behaviors of *TH-Cre* mice resembled those of *Erbb4*$^{loxp/loxp}$ mice (data not shown), and both lines were used as controls. All experiments were performed in a double-blind fashion.

Open field test

Open field tests were performed in an open field chamber (50 cm × 50 cm) equipped with infrared sensors (CCTV lens) in a room with dim light. Mice could freely explore the novel environment for 10 min, and their movements were traced and analyzed simultaneously using viewpoint application manager software (VideoTrack 3.10). Total distance, speed, and immobility time were analyzed. The open field chamber was cleaned with 70% ethanol and wiped with paper towels between tests.

Elevated plus maze test

Elevated plus maze (EPM) tests were performed in a dimly lit room. The maze was elevated 70 cm above the floor and consisted of two closed arms (5 × 30 cm) surrounded by 15-cm-high plastic walls and two open arms (5 × 30 cm). For

testing, a mouse was placed in the center (5 × 5 cm) of the maze and allowed to explore for 5 min. Mouse movements were recorded and analyzed using Mobile Datum recording and analysis software. The amount of time spent in and number of entries into the open arms and closed arms were measured. The maze was cleaned with 70% ethanol and wiped with paper towels after each test.

Forced swim test

Forced swim tests were performed in a room with normal light. Mice were placed in a transparent plastic cylinder (diameter: 12 cm; height: 30 cm) containing 20–24°C water at 15-cm depth. During the 6-min test period, the mice were monitored using a video camera (Mobile Datum) from the side. Total time spent, immobility time, and latency to first immobility were analyzed by an observer off-line, who was blinded to the experimental treatments. After the 6-min test period, the cylinders were cleaned with 70% ethanol and wiped with paper towels. The water in the cylinder was changed for each new mouse.

Sucrose preference test

Mice were single-housed for 1 week with a normal drinking water bottle. The bottle was then replaced with two identical bottles (bottle “A” and bottle “B”) filled with drinking water for 2 d (W/W). The positions of bottle A and bottle B were switched daily to avoid place preference. Bottle A and bottle B were then filled with drinking water alone and drinking water with 2% sucrose, respectively, for 2 d (W/S) and switched after 24 h. The consumption of the solutions in bottle A and bottle B were measured by weighing, and the preference for sucrose was calculated as the ratio of consumption of the sucrose solution to that of both the water and sucrose solutions during the 2 d of testing.

Prepulse inhibition

During the PPI test, mice were subjected to 20 startle trials (120 dB, 20 ms), 10 pre-pulse/startle trials (pre-pulse duration, 20 ms; intensities, 75, 80, and 85 dB; interstimulus intervals, 100 ms; and 20 ms 120 dB startle stimulus), 15 pre-pulse trials (5 for 75, 80, and 85 dB each), and five background noise trials (65 dB), for a total of 70 trials. Different trial types were presented pseudorandomly. No two consecutive trials were identical except for five consecutive startle trials at the beginning and end of each session, which were not used for PPI analysis. Mouse movement was measured during 65 ms after startle stimulus onset (sampling frequency 1 kHz). PPI (%) was calculated according to the formula: (100 − (startle amplitude on pre-pulse-startle trials / startle amplitude on startle pulse alone trials) × 100).

Drug treatment

Mice were treated for 10 d with lithium chloride (600 mg L^{-1}) in drinking water and were then subjected to behavioral tests or sacrificed for Western blotting or patch clamp experiments (Dehpour et al., 2002; Roybal et al., 2007). Prazosin and SCH23390 were injected (i.p.) 30 min before the experiment.

Quantification and statistical analysis

The samples were randomly assigned to each group and restricted randomization was applied. The investigator was blinded to group allocation and when assessing outcome in the all behavioral tests and immunocytochemistry tests. For the electrophysiology experiments, the investigator was blinded when assessing outcome. For quantification, values from three independent experiments with at least three biological replicates were used. For behavioral assays, all population values appeared normally distributed, and variance was similar between groups. Sample size was calculated according to the preliminary experimental results and the formula: $N = [(Z_{\alpha/2} + Z_{\beta})\sigma / \delta]^2(Q1^{-1} + Q2^{-1})$, where $\alpha = 0.05$ significance level, $\beta = 0.2$, power = 1-β, δ is the difference between means of two samples, and Q is the sample fraction. All data are presented as means ± s.e.m. and were analyzed using Two-tailed Student's t-test, one-way analysis of variance (ANOVA), two-way ANOVA, or two-way repeated-measures ANOVA. The Kolmogorov–Smirnov test (K–S test) was used to compare the interspike interval distributions, as specified in each figure legend and Supplementary Tables 1–4. Grubbs' test are used to detect an outlier. All data were analyzed using Origin8.0 (OriginLab) and Clampfit 10.2 (AxonInstruments). Data were exported into Illustrator CS5 (Adobe Systems) for preparation of figures.

Acknowledgements

We thank Nick Spitzer (University of California at San Diego) for manuscript suggestions. We are grateful to Y.Q. Ding (Tongji University) and X.Q Chen (Institute of Neuroscience, Zhejiang University) for providing mouse lines or experimental facilities. We express our thanks to L. Wang (Zhejiang University) for technical assistance.

Additional information

Funding

Funder	Grant reference	Author
National Key R & D Program of China	2016YFA0501003	Xiao-Ming Li
National Natural Science Foundation of China	91432306	Xiao-Ming Li
National Natural Science Foundation of China	31430034	Xiao-Ming Li
National Natural Science Foundation of China	81221003	Xiao-Ming Li
National Natural Science Foundation of China	31700904	Shu-Xia Cao
Zhejiang Provincial Natural Science Foundation of China	LY17C090004	Hong Lian

The funders had no role in study design, data collection and interpretation, or decision to submit this work for publication.

Author contributions

S-XC conducted the experiments, collected and analyzed the data, and wrote the manuscript; YZ conducted the experiments and collected the data; S-XC, PS, H-YH, and BH contributed to *in vivo* microdialysis; H-YG conducted part of the behavioral experiments; X-YH, A-MB, S-MD, J-MY, and T-MG contributed experimental and manuscript suggestions; HL conducted experiments, supervised the project, and wrote the manuscript; X-ML supervised the project and wrote the manuscript.

Ethics

Animal experimentation: The care and use of the mice were reviewed and approved by the Animal Advisory Committee at Zhejiang University. Every effort was made to minimize suffering.

References

Arey RN, Enwright JF, Spencer SM, Falcon E, Ozburn AR, Ghose S, Tamminga C, and McClung CA. 2013. An important role for Cholecystokinin, a CLOCK target gene, in the development and treatment of manic-like behaviors. *Molecular Psychiatry*. doi: 10.1038/mp.2013.12.

Aumann TD, Egan K, Lim J, Boon WC, Bye CR, Chua HK, Baban N, Parish CL, Bobrovskaya L, Dickson P, and Horne MK. 2011. Neuronal activity regulates expression of tyrosine hydroxylase in adult mouse substantia nigra pars compacta neurons. *J Neurochem* 116: 646-658. doi: 10.1111/j.1471-4159.2010.07151.x.

Bean JC, Lin TW, Sathyamurthy A, Liu F, Yin DM, Xiong WC, and Mei L. 2014. Genetic labeling reveals novel cellular targets of schizophrenia susceptibility gene: distribution of GABA and non-GABA ErbB4-positive cells in adult mouse brain. *J Neurosci* 34: 13549-13566. doi: 10.1523/JNEUROSCI.2021-14.2014.

Benarroch EE. 2009. The locus ceruleus norepinephrine system: functional organization and potential clinical significance. *Neurology* 73: 1699-1704. doi: 10.1212/WNL.0b013e3181c2937c.

Bernard R, Kerman IA, Thompson RC, Jones EG, Bunney WE, Barchas JD, Schatzberg AF, Myers RM, Akil H, and Watson SJ. 2011. Altered expression of glutamate signaling, growth factor, and glia genes in the locus coeruleus of patients with major depression. *Mol Psychiatry* 16: 634-646. doi: 10.1038/mp.2010.44.

Berridge CW, and Waterhouse BD. 2003. The locus coeruleus–noradrenergic system: modulation of behavioral state and state-dependent cognitive processes. *Brain Research Reviews* 42: 33-84. doi: 10.1016/s0165-0173(03)00143-7.

Bielau H, Brisch R, Bernard-Mittelstaedt J, Dobrowolny H, Gos T, Baumann B, Mawrin C, Bernstein HG, Bogerts B, and Steiner J. 2012. Immunohistochemical evidence for impaired nitric oxide signaling of the locus coeruleus in bipolar disorder. *Brain Res* 1459: 91-99. doi: 10.1016/j.brainres.2012.04.022.

Bjarnadottir M, Misner DL, Haverfield-Gross S, Bruun S, Helgason VG, Stefansson H, Sigmundsson A, Firth DR, Nielsen B, Stefansdottir R*, et al.* 2007. Neuregulin1 (NRG1) signaling through Fyn modulates NMDA receptor phosphorylation: differential synaptic function in NRG1+/- knock-outs compared with wild-type mice. *J Neurosci* 27: 4519-4529. doi: 10.1523/jneurosci.4314-06.2007.

Bjorklund A, and Dunnett SB. 2007. Dopamine neuron systems in the brain: an update. *Trends Neurosci* 30: 194-202. doi: 10.1016/j.tins.2007.03.006.

Borodovitsyna O, Flamini M, and Chandler D. 2017. Noradrenergic modulation of cognition in health and disease. *Neural Plast* 2017: 6031478. doi: 10.1155/2017/6031478.

Carboni E, Tanda GL, Frau R, and Di Chiara G. 1990. Blockade of the noradrenaline carrier increases extracellular dopamine concentrations in the prefrontal cortex: evidence that dopamine is taken up in vivo by noradrenergic terminals. *J Neurochem* 55: 1067-1070. doi: 10.1111/j.1471-4159.1990.tb04599.x.

Chandler DJ, Gao WJ, and Waterhouse BD. 2014. Heterogeneous organization of the locus coeruleus projections to prefrontal and motor cortices. *Proc Natl Acad Sci U S A* 111: 6816-6821. doi: 10.1073/pnas.1320827111.

Chen P, Chen J, Huang K, Ji W, Wang T, Li T, Wang Y, Wang H, He L, Feng G, and Shi Y. 2012. Analysis of association between common SNPs in ErbB4 and bipolar affective disorder, major depressive disorder and schizophrenia in the Han Chinese population. *Prog Neuropsychopharmacol Biol Psychiatry* 36: 17-21. doi: 10.1016/j.pnpbp.2011.09.011.

Chen YJ, Zhang M, Yin DM, Wen L, Ting A, Wang P, Lu YS, Zhu XH, Li SJ, Wu CY*, et al.* 2010. ErbB4 in parvalbumin-positive interneurons is critical for neuregulin 1 regulation of long-term potentiation. *Proc Natl Acad Sci U S A* 107: 21818-21823. doi: 10.1073/pnas.1010669107.

Chevalier J, Derkinderen P, Gomes P, Thinard R, Naveilhan P, Vanden Berghe P, and Neunlist M. 2008. Activity-dependent regulation of tyrosine hydroxylase expression in the enteric nervous system. *J Physiol* 586: 1963-1975. doi: 10.1113/jphysiol.2007.149815.

Chong VZ, Thompson M, Beltaifa S, Webster MJ, Law AJ, and Weickert CS. 2008. Elevated neuregulin-1 and ErbB4 protein in the prefrontal cortex of schizophrenic patients. *Schizophr Res* 100: 270-280. doi: 10.1016/j.schres.2007.12.474.

Cosgrove VE, Kelsoe JR, and Suppes T. 2015. Toward a valid animal model of bipolar disorder: how the research domain criteria help bridge the clinical-basic science divide. *Biological Psychiatry* 79: 62-70. doi: 10.1016/j.biopsych.2015.09.002.

Craddock N, and Sklar P. 2009. Genetics of bipolar disorder: successful start to a long journey. *Trends Genet* 25: 99-105. doi: 10.1016/j.tig.2008.12.002.

Del Pino I, Garcia-Frigola C, Dehorter N, Brotons-Mas JR, Alvarez-Salvado E, Martinez de Lagran M, Ciceri G, Gabaldon MV, Moratal D, Dierssen M*, et al.* 2013. Erbb4 deletion from fast-spiking interneurons causes schizophrenia-like phenotypes. *Neuron* 79: 1152-1168. doi: 10.1016/j.neuron.2013.07.010.

Devoto P, Flore G, Saba P, Fa M, and Gessa GL. 2005. Stimulation of the locus coeruleus elicits noradrenaline and dopamine release in the medial prefrontal and parietal cortex. *J Neurochem* 92: 368-374. doi: 10.1111/j.1471-4159.2004.02866.x.

Dickinson SL, Gadie B, and Tulloch IF. 1988. Alpha 1- and alpha 2-adrenoreceptor antagonists differentially influence locomotor and stereotyped behaviour induced by d-amphetamine and apomorphine in the rat. *Psychopharmacology (Berl)* 96: 521-527. doi.

Fisahn A, Neddens J, Yan L, and Buonanno A. 2009. Neuregulin-1 modulates hippocampal gamma oscillations: implications for schizophrenia. *Cereb Cortex* 19: 612-618. doi: 10.1093/cercor/bhn107.

Gary Aston-Jones aJDC. 2005. An Integrative Theory of Locus Coeruleus-Norepinephrine Function Adaptive Gain and Optimal Performance.pdf. *Annu Rev Neurosci* 28: 403. doi: 10.1146/.

Gelman DM, Noain D, Avale ME, Otero V, Low MJ, and Rubinstein M. 2003. Transgenic mice engineered to target Cre/loxP-mediated DNA recombination into catecholaminergic neurons. *Genesis* 36: 196-202. doi: 10.1002/gene.10217.

Gerecke. 2001. ErbB Transmembrane Tyrosine Kinase.pdf. doi.

Goes FS, Rongione M, Chen YC, Karchin R, Elhaik E, Bipolar Genome S, and Potash JB. 2011. Exonic DNA sequencing of ERBB4 in bipolar disorder. *PLoS One* 6: e20242. doi: 10.1371/journal.pone.0020242.

Gong S, Doughty M, Harbaugh CR, Cummins A, Hatten ME, Heintz N, and Gerfen CR. 2007. Targeting Cre recombinase to specific neuron populations with bacterial artificial chromosome constructs. *J Neurosci* 27: 9817-9823. doi: 10.1523/JNEUROSCI.2707-07.2007.

Gouvea ES, Ota VK, Noto C, Santoro ML, Spindola LM, Moretti PN, Carvalho CM, Xavier G, Rios AC, Sato JR*, et al.* 2016. Gene expression alterations related to mania and psychosis in peripheral blood of patients with a first episode of psychosis. *Transl Psychiatry* 6: e908. doi: 10.1038/tp.2016.159.

Guiard BP, El Mansari M, Merali Z, and Blier P. 2008. Functional interactions between dopamine, serotonin and norepinephrine neurons: an in-vivo electrophysiological study in rats with monoaminergic lesions. *Int J Neuropsychopharmacol* 11: 625-639. doi: 10.1017/s1461145707008383.

Hahn CG, Wang HY, Cho DS, Talbot K, Gur RE, Berrettini WH, Bakshi K, Kamins J, Borgmann-Winter KE, Siegel SJ*, et al.* 2006. Altered neuregulin 1-erbB4 signaling contributes to NMDA receptor hypofunction in schizophrenia. *Nat Med* 12: 824-828. doi: 10.1038/nm1418.

Han K, Holder JL, Jr., Schaaf CP, Lu H, Chen H, Kang H, Tang J, Wu Z, Hao S, Cheung SW*, et al.* 2013. SHANK3 overexpression causes manic-like behaviour with unique pharmacogenetic properties. *Nature* 503: 72-77. doi: 10.1038/nature12630.

Harrison PJ, Geddes JR, and Tunbridge EM. 2017. The Emerging Neurobiology of Bipolar Disorder. *Trends Neurosci*. doi: 10.1016/j.tins.2017.10.006.

Holden C. 2008. Poles apart. *Science* 321: 193-195. doi: 10.1126/science.321.5886.193.

Jedema HP, and Grace AA. 2004. Corticotropin-releasing hormone directly activates noradrenergic neurons of the locus ceruleus recorded in vitro. *J Neurosci* 24: 9703-9713. doi: 10.1523/JNEUROSCI.2830-04.2004.

Jodo E, and Aston-Jones G. 1997. Activation of locus coeruleus by prefrontal cortex is mediated by excitatory amino acid inputs. *Brain Res* 768: 327-332. doi: 10.1016/S0006-8993(97)00703-8.

Jope RS. 1999. Anti-bipolar therapy: mechanism of action of lithium. *Mol Psychiatry* 4: 117-128. doi.

Kato T. 2008. Molecular neurobiology of bipolar disorder a disease of 'mood-stabilizing neurons?.pdf. *Trends in Neurosciences* 31: 495. doi: 10.1016/j.tins.2008.07.007.

Kirshenbaum GS, Clapcote SJ, Duffy S, Burgess CR, Petersen J, Jarowek KJ, Yucel YH, Cortez MA, Snead OC, 3rd, Vilsen B*, et al.* 2011. Mania-like behavior induced by genetic dysfunction of the neuron-specific Na+,K+-ATPase alpha3 sodium pump. *Proc Natl Acad Sci U S A* 108: 18144-18149. doi: 10.1073/pnas.1108416108.

Kurita M. 2016. Noradrenaline plays a critical role in the switch to a manic episode and treatment of a depressive episode. *Neuropsychiatr Dis Treat* 12: 2373-2380. doi: 10.2147/NDT.S109835.

Lammel S, Steinberg EE, Foldy C, Wall NR, Beier K, Luo L, and Malenka RC. 2015. Diversity of transgenic mouse models for selective targeting of midbrain dopamine neurons. *Neuron* 85: 429-438. doi: 10.1016/j.neuron.2014.12.036.

Langer SZ. 1980. Presynaptic regulation of the release of catecholamines. *Pharmacol Rev* 32: 337-362. doi.

Lew JY, Garcia-Espana A, Lee KY, Carr KD, Goldstein M, Haycock JW, and Meller E. 1999. Increased site-specific phosphorylation of tyrosine hydroxylase accompanies stimulation of enzymatic activity induced by cessation of dopamine neuronal activity. *Mol Pharmacol* 55: 202-209. doi: 10.1124/mol.55.2.202.

Li KX, Lu YM, Xu ZH, Zhang J, Zhu JM, Zhang JM, Cao SX, Chen XJ, Chen Z, Luo JH*, et al.* 2012. Neuregulin 1 regulates excitability of fast-spiking neurons through Kv1.1 and acts in epilepsy. *Nat Neurosci* 15: 267-273. doi: 10.1038/nn.3006.

Lindeberg J, Usoskin D, Bengtsson H, Gustafsson A, Kylberg A, Soderstrom S, and Ebendal T. 2004. Transgenic expression of Cre recombinase from the tyrosine hydroxylase locus. *Genesis* 40: 67-73. doi: 10.1002/gene.20065.

Maas JW, Dekirmenjian H, and Fawcett J. 1971. Catecholamine metabolism, depression and stress. *Nature* 230: 330-331. doi.

Madisen L, Zwingman TA, Sunkin SM, Oh SW, Zariwala HA, Gu H, Ng LL, Palmiter RD, Hawrylycz MJ, Jones AR*, et al.* 2010. A robust and high-throughput Cre reporting and characterization system for the whole mouse brain. *Nature neuroscience* 13: 133-140. doi: 10.1038/nn.2467.

Manji HK, Quiroz JA, Payne JL, Singh J, Lopes BP, Viegas JS, and Zarate CA. 2003. The underlying neurobiology of bipolar disorder. *World Psychiatry* 2: 136-146. doi.

Mather M, and Harley CW. 2016. The Locus Coeruleus: Essential for Maintaining Cognitive Function and the Aging Brain. *Trends Cogn Sci* 20: 214-226. doi: 10.1016/j.tics.2016.01.001.

Mei L, and Nave KA. 2014. Neuregulin-ERBB signaling in the nervous system and neuropsychiatric diseases. *Neuron* 83: 27-49. doi: 10.1016/j.neuron.2014.06.007.

Mei L, and Xiong WC. 2008. Neuregulin 1 in neural development, synaptic plasticity and schizophrenia. *Nat Rev Neurosci* 9: 437-452. doi: 10.1038/nrn2392.

Moret C, and Briley M. 2011. The importance of norepinephrine in depression. *Neuropsychiatr Dis Treat* 7: 9-13. doi: 10.2147/NDT.S19619.

Neophytou SI, Aspley S, Butler S, Beckett S, and Marsden CA. 2001. Effects of lesioning noradrenergic neurones in the locus coeruleus on conditioned and unconditioned aversive behaviour in the rat. *Prog Neuropsychopharmacol Biol Psychiatry* 25: 1307-1321. doi.

Nestler EJ, and Hyman SE. 2010. Animal models of neuropsychiatric disorders. *Nat Neurosci* 13: 1161-1169. doi: 10.1038/nn.2647.

Pamphlett R. 2014. Uptake of environmental toxicants by the locus ceruleus: a potential trigger for neurodegenerative, demyelinating and psychiatric disorders. *Med Hypotheses* 82: 97-104. doi: 10.1016/j.mehy.2013.11.016.

Pitcher GM, Kalia LV, Ng D, Goodfellow NM, Yee KT, Lambe EK, and Salter MW. 2011. Schizophrenia susceptibility pathway neuregulin 1-ErbB4 suppresses Src upregulation of NMDA receptors. *Nat Med* 17: 470-478. doi: 10.1038/nm.2315.

Post RM, Gordon EK, Goodwin FK, and Bunney WE, Jr. 1973. Central norepinephrine metabolism in affective illness: MHPG in the cerebrospinal fluid. *Science* 179: 1002-1003. doi.

Post RM, Lake CR, Jimerson DC, Bunney WE, Wood JH, Ziegler MG, and Goodwin FK. 1978. Cerebrospinal fluid norepinephrine in affective illness. *Am J Psychiatry* 135: 907-912. doi.

Pozzi L, Invernizzi R, Cervo L, Vallebuona F, and Samanin R. 1994. Evidence that extracellular concentrations of dopamine are regulated by noradrenergic neurons in the frontal cortex of rats. *J Neurochem* 63: 195-200. doi: 10.1046/j.1471-4159.1994.63010195.x.

Prickaerts J, Moechars D, Cryns K, Lenaerts I, van Craenendonck H, Goris I, Daneels G, Bouwknecht JA, and Steckler T. 2006. Transgenic mice overexpressing glycogen synthase kinase 3beta: a putative model of hyperactivity and mania. *J Neurosci* 26: 9022-9029. doi: 10.1523/JNEUROSCI.5216-05.2006.

Ross JA, McGonigle P, and Van Bockstaele EJ. 2015. Locus Coeruleus, norepinephrine and Abeta peptides in Alzheimer's disease. *Neurobiol Stress* 2: 73-84. doi: 10.1016/j.ynstr.2015.09.002.

Roybal K, Theobold D, Graham A, DiNieri JA, Russo SJ, Krishnan V, Chakravarty S, Peevey J, Oehrlein N, Birnbaum S*, et al.* 2007. Mania-like behavior induced by disruption of CLOCK. *Proc Natl Acad Sci U S A* 104: 6406-6411. doi: 10.1073/pnas.0609625104.

Salvadore G, Quiroz JA, Machado-Vieira R, Henter ID, Manji HK, and Zarate CA. 2010. The Neurobiology of the Switch Process in Bipolar Disorder: a Review. *The Journal of clinical psychiatry* 71: 1488-1501. doi: 10.4088/JCP.09r05259gre.

Sara SJ. 2009. The locus coeruleus and noradrenergic modulation of cognition. *Nat Rev Neurosci* 10: 211-223. doi: 10.1038/nrn2573.

Saul MC, Gessay GM, and Gammie SC. 2012. A new mouse model for mania shares genetic correlates with human bipolar disorder. *PLoS One* 7: e38128. doi: 10.1371/journal.pone.0038128.

Savitt JM, Jang SS, Mu W, Dawson VL, and Dawson TM. 2005. Bcl-x is required for proper development of the mouse substantia nigra. *J Neurosci* 25: 6721-6728. doi: 10.1523/JNEUROSCI.0760-05.2005.

Schloesser RJ, Martinowich K, and Manji HK. 2012. Mood-stabilizing drugs: mechanisms of action. *Trends Neurosci* 35: 36-46. doi: 10.1016/j.tins.2011.11.009.

Shaltiel G, Maeng S, Malkesman O, Pearson B, Schloesser RJ, Tragon T, Rogawski M, Gasior M, Luckenbaugh D, Chen G, and Manji HK. 2008. Evidence for the involvement of the kainate receptor subunit GluR6 (GRIK2) in mediating behavioral displays related to behavioral symptoms of mania. *Mol Psychiatry* 13: 858-872. doi: 10.1038/mp.2008.20.

Shamir A, Kwon OB, Karavanova I, Vullhorst D, Leiva-Salcedo E, Janssen MJ, and Buonanno A. 2012. The importance of the NRG-1/ErbB4 pathway for synaptic plasticity and behaviors associated with psychiatric disorders. *J Neurosci* 32: 2988-2997. doi: 10.1523/JNEUROSCI.1899-11.2012.

Skirzewski M, Karavanova I, Shamir A, Erben L, Garcia-Olivares J, Shin JH, Vullhorst D, Alvarez VA, Amara SG, and Buonanno A. 2017. ErbB4 signaling in dopaminergic axonal projections increases extracellular dopamine levels and regulates spatial/working memory behaviors. *Mol Psychiatry*. doi: 10.1038/mp.2017.132.

Somogyi J, and Llewellyn-Smith IJ. 2001. Patterns of colocalization of GABA, glutamate and glycine immunoreactivities in terminals that synapse on dendrites of noradrenergic neurons in rat locus coeruleus. *Eur J Neurosci* 14: 219-228. doi: 10.1046/j.0953-816x.2001.01638.x.

578 Starke K. 2001. Presynaptic autoreceptors in the third decade: focus on alpha2-adrenoceptors. *J Neurochem* 78: 685-
579 693. doi: 10.1046/j.1471-4159.2001.00484.x.
580 Tan GH, Liu YY, Hu XL, Yin DM, Mei L, and Xiong ZQ. 2012. Neuregulin 1 represses limbic epileptogenesis through ErbB4
581 in parvalbumin-expressing interneurons. *Nat Neurosci* 15: 258-266. doi: 10.1038/nn.3005.
582 Wiste AK, Arango V, Ellis SP, Mann JJ, and Underwood MD. 2008. Norepinephrine and serotonin imbalance in the locus
583 coeruleus in bipolar disorder. *Bipolar Disord* 10: 349-359. doi: 10.1111/j.1399-5618.2007.00528.x.
584 Yamamoto BK, and Novotney S. 1998. Regulation of extracellular dopamine by the norepinephrine transporter. *J*
585 *Neurochem* 71: 274-280. doi: 10.1046/j.1471-4159.1998.71010274.x.
586 Zigmond RE, Schwarzschild MA, and Rittenhouse AR. 1989. Acute regulation of tyrosine hydroxylase by nerve activity
587 and by neurotransmitters via phosphorylation. *Annu Rev Neurosci* 12: 415-461. doi:
588 10.1146/annurev.ne.12.030189.002215.

589

Figure legends

Figure 1. ErbB4 is primarily deleted in NE neurons of the LC in *TH-Cre;Erbb4*$^{loxp/loxp}$ mice. **A**, Representative micrographs of Cre/Tomato distribution (red) in the locus coeruleus (LC), ventral tegmental area (VTA), and substantia nigra pars compacta (SNC). Slices were obtained from Ai9;*TH-Cre* mice and stained with antibody to TH (green), a marker of NE and dopaminergic neurons. Scale bar, 50 μm. **B**, Colocalization of TH and Cre/Tomato. Three mice were studied, with three slices chosen for each mouse. **C**, Genotyping of *TH-Cre;Erbb4*$^{loxp/loxp}$ mice. The *Erbb4* primers generated a 363-base pair (bp) product for the wild-type allele or a 500-bp product for the loxP-flanked allele. The *TH-Cre* primers generated a band between 300 and 400 bp. **D**, **E**, Quantification of the fold change in ErbB4 protein expression relative to control mice. Unpaired two-tailed Student's t-test. Data are expressed as means ± s.e.m. ** $p < 0.01$. **F**, Specific deletion of ErbB4 in NE neurons of the LC. Sections from *TH-Cre* mice and *TH-Cre;Erbb4*$^{loxp/loxp}$ mice were stained with ErbB4-specific antibody and TH-specific antibody. Sections were also stained with DAPI to indicate nuclei. Scale bar, 10 μm.

Figure 2. Increased spontaneous firing of LC-NE neurons, extracellular norepinephrine, and intracellular TH phosphorylation in *TH-Cre;Erbb4*$^{loxp/loxp}$ mice. **A**, **B**, Representative firing of LC-NE neurons from control (black) and *TH-Cre;Erbb4*$^{loxp/loxp}$ mice (red). **C**, Spontaneous firing frequency of LC-NE neurons increased in *TH-Cre;Erbb4*$^{loxp/loxp}$ mice. n = 11 from three mice (control); n = 13 from three mice (*TH-Cre;Erbb4*$^{loxp/loxp}$). **D**, Interspike intervals were calculated over 2 min of firing from each neuron. Interspike intervals were decreased in *TH-Cre;Erbb4*$^{loxp/loxp}$ mice compared with control mice. n = 11 from three mice (control); n = 13 from three mice (*TH-Cre;Erbb4*$^{loxp/loxp}$). Two-sample Kolmogorov-Smirnov test and data in (D) are presented in a cumulative frequency plot. **** $p < 0.0001$. **E**, **F**, Protein levels of TH-Ser40 were increased in the LC of *TH-Cre;Erbb4*$^{loxp/loxp}$ mice. NET, norepinephrine reuptake transporter; DBH, dopamine beta-hydroxylase; S-COMT, soluble catechol-o-methyltransferase; MB-COMT, membrane-binding form of COMT. **G**, **H**, No significant change was detected in the dopaminergic neurons clustered in the midbrain (VTA and SNC). **I**, **J**, *In vivo* microdialysis and HPLC data suggested that norepinephrine and dopamine levels were significantly increased in *TH-Cre;Erbb4*$^{loxp/loxp}$ mice. Standard curves are presented in Figures 2-figure supplement 2. n = 6 mice (control); n = 6 mice (*TH-Cre;Erbb4*$^{loxp/loxp}$). Unpaired two-tailed Student's t-test. Data are expressed as means ± s.e.m. * $p < 0.05$.

Figure 3. NMDA receptor mediates hyperexcitability of LC-NE neurons in *TH-Cre;Erbb4*$^{loxp/loxp}$ mice. **A**, **B,** Protein levels of NMDA receptor subunit NR2B were increased in the LC of *TH-Cre;Erbb4*$^{loxp/loxp}$ mice. Unpaired two-tailed Student's t-test. Data are expressed as means ± s.e.m. * $p < 0.05$. **C**, Representative firing of LC-NE neurons from control and *TH-Cre;Erbb4*$^{loxp/loxp}$ mice untreated or treated with APV (50 μM), a NMDA receptor antagonist. **D**, Spontaneous firing frequency of LC-NE neurons was rescued by APV (50 μM) in *TH-Cre;Erbb4*$^{loxp/loxp}$ mice. n = 13 from three mice (*TH-Cre;Erbb4*$^{loxp/loxp}$); n = 20 from three mice (*TH-Cre;Erbb4*$^{loxp/loxp}$+APV). Two-way ANOVA. Data are expressed as means ± s.e.m. * $p < 0.05$. **E**, Interspike intervals were significantly rescued by APV (50 μM) in *TH-Cre;Erbb4*$^{loxp/loxp}$ mice. n = 13 from three mice (*TH-Cre;Erbb4*$^{loxp/loxp}$); n = 20 from three mice (*TH-Cre;Erbb4*$^{loxp/loxp}$+APV). Two-sample Kolmogorov-Smirnov test and data in (**E**) are presented in a cumulative frequency plot. *** $p < 0.001$.

Figure 4. *TH-Cre;Erbb4*$^{loxp/loxp}$ mice show mania-like behaviors. **A**, Representative trajectories of control and *TH-Cre;Erbb4*$^{loxp/loxp}$ mice. We defined high speed (red line) as > 10 cm/s, immobility as < 2 cm/s, and low speed (green line) as 2–10 cm/s. **B**, **C**,

Locomotor activity (**B**) and speed (**C**) of control and *TH-Cre;Erbb4*$^{loxp/loxp}$ mice in open field tests. **D**, **E**, Distance (**D**) and duration (**E**) traveled at high speed (HS). **F**, Immobility time during open field tests decreased in *TH-Cre;Erbb4*$^{loxp/loxp}$ mice. **G**, Examples of the performance of control and *TH-Cre;Erbb4*$^{loxp/loxp}$ mice in the EPM test. C, closed arm; O, open arm. **H**, **I**, Performance of control and *TH-Cre;Erbb4*$^{loxp/loxp}$ mice in the EPM test. **J**, **K**, Immobility time (**J**) and latency to first surrender (**K**) in the forced swim test. **L**, Sucrose preference of control and *TH-Cre;Erbb4*$^{loxp/loxp}$ mice. Water (w). Sucrose (s). Unpaired two-tailed Student's t-test. Data are expressed as means ± s.e.m. * $p < 0.05$, ** $p < 0.01$, *** $p < 0.001$, **** $p < 0.0001$. n.s., not significant.

Figure 5. Specific ablation of ErbB4 in the LC is sufficient to cause mania-like behaviors. **A**, Illustration of bilateral viral injection of AAV-Cre-GFP in the mouse LC. LC sections were examined for Cre/GFP (green) 5 weeks after stereotaxic microinjection of AAV-Cre-GFP into the LC of *Erbb4*$^{loxp/loxp}$ mice; antibody staining for TH is shown in red. Scale bars, 50 μm. Cartogram is presented in Figure S5. **B**, ErbB4 expression was significantly decreased in *Erbb4*$^{loxp/loxp}$ mice after AAV-Cre-GFP injection. **C**, **D**, Locomotor activity (**C**) and speed (**D**) of mice injected with AAV-GFP or AAV-Cre-GFP in the open field test. **E-G**, Distance (**E**) and duration (**F**) traveled at HS and immobility time (**G**) of mice in the open field test after viral injection. **H**, **I**, Percentage of time (**H**) and entries (**I**) into the open arms by mice injected with AAV-GFP or AAV-Cre-GFP in the EPM test. **J**, **K**, Immobility time (**J**) and latency to first surrender (**K**) in the forced swim test with AAV-GFP or AAV-Cre-GFP injection. **L**, Sucrose preference of mice injected with AAV-GFP or AAV-Cre-GFP. Unpaired two-tailed Student's t-test. Data are expressed as means ± s.e.m. * $p < 0.05$, ** $p < 0.01$, **** $p < 0.0001$.

Figure 6. Lithium rescued the behavioral, molecular, and electrophysiological phenotypes of *TH-Cre;Erbb4*$^{loxp/loxp}$ mice. **A**, **B** Locomotor activity (**A**) and speed (**B**) in the open field test. **C-E**, Distance (**C**) and duration (**D**) traveled at HS and immobility time (**E**) after lithium treatment. **F**, **G** Percentage of time (**F**) and entries (**G**) into open arms by *TH-Cre;Erbb4*$^{loxp/loxp}$ mice with and without lithium in the EPM test. **H**, **I** Immobility time (**H**) and latency to first surrender (**I**) in forced swim test. **J**, Sucrose preference of *TH-Cre;Erbb4*$^{loxp/loxp}$ mice treated with lithium. **K**, Western blots of LC samples from *TH-Cre;Erbb4*$^{loxp/loxp}$ mice with and without lithium treatment. **L**, Protein level of TH-Ser40 in the LC after lithium treatment. Protein levels of TH, s-COMT, and MB-COMT were not significantly changed in the LC after lithium treatment. TH, tyrosine hydroxylase; S-COMT, soluble catechol-o-methyltransferase; MB-COMT, membrane-binding form of COMT. **M**, Spontaneous firing of LC-NE neurons after lithium treatment. n = 13 from three mice (*TH-Cre;Erbb4*$^{loxp/loxp}$); n = 15 from three mice (*TH-Cre;Erbb4*$^{loxp/loxp}$ + lithium). **N**, Interspike intervals after lithium treatment. n = 13 from three mice (*TH-Cre;Erbb4*$^{loxp/loxp}$); n = 15 from three (*TH-Cre;Erbb4*$^{loxp/loxp}$ + lithium). Two-way ANOVA. Data are expressed as means ± s.e.m. Two-sample Kolmogorov-Smirnov test and data in (**N**) are presented as a cumulative frequency plot. * $p < 0.05$, ** $p < 0.01$, **** $p < 0.0001$. n.s., not significant.

Figure 7. Increase in both norepinephrine and dopamine contribute to mania-like behaviors. **A**, **B**, Locomotor activity (**A**) and speed (**B**) of *TH-Cre;Erbb4*$^{loxp/loxp}$ mice treated with saline (sal), prazosin, or SCH23390 in open field test. **C**, **D**, Distance (**C**) and duration (**D**) at HS in open field test. **E**, Immobility time in open field test. **F**, **G**, Time (**F**) and entries (**G**) in open arms in EPM test. **H**, **I**, Immobility time (**H**) and latency to first surrender (**I**) in forced swim tests. **J**, Sucrose preference of *TH-Cre;Erbb4*$^{loxp/loxp}$ mice after prazosin or SCH23390 treatment. One-way ANOVA and Tukey's multiple comparison test. Data are expressed as means ± s.e.m. * $p < 0.05$, ** $p < 0.01$, *** $p < 0.001$, **** $p < 0.0001$. n.s., not significant.

658

Supplementary figure legends

Figure 1-figure supplement 1. Cre/GFP was primarily expressed in NE neurons of the LC in Ai3;*TH-Cre* mice. **A**, Representative micrographs of Cre/GFP distribution (green) in Ai3;*TH-Cre* mice. Locus coeruleus (LC), ventral tegmental area (VTA), and substantia nigra pars compacta (SNC) slices were obtained from Ai3;*TH-Cre* mice and stained with antibody to TH (red), a marker of NE and dopaminergic neurons. Scale bar, 50 μm. **B**, Cartogram of Cre expression in TH-positive neurons in the LC, VTA, and SNC. Three mice were studied, with three slices for each mouse.

Figure 1-figure supplement 2. ErbB4 was primarily deleted in the LC of *TH-Cre;Erbb4*$^{loxp/loxp}$ mice. Shown are representative Western blots of the ErbB4 protein (180 kDa) in *TH-Cre;Erbb4*$^{loxp/loxp}$ mice. *Erbb4*$^{loxp/loxp}$ mice and *TH-Cre* mice were used as controls.

Figure 1-figure supplement 3. No obvious differences were detected in cell density or soma size of LC neurons between control and *TH-Cre;Erbb4*$^{loxp/loxp}$ mice. **A**, Representative micrographs of LC neurons in the dorsal and ventral parts of the LC in control and *TH-Cre;Erbb4*$^{loxp/loxp}$ mice. Coronal LC slices were obtained from control and *TH-Cre;Erbb4*$^{loxp/loxp}$ mice and were stained with antibody to TH (green), a marker of NE and dopaminergic neurons. Scale bar, 50 μm. **B**, **C**, Cell density and soma size of LC neurons did not differ significantly between control and *TH-Cre;Erbb4*$^{loxp/loxp}$ mice. Unpaired two-tailed Student's t-test. Data are expressed as means ± s.e.m. n.s., not significant.

Figure 2-figure supplement 1. Representative Western blots of TH and COMT in the LC of control and *TH-Cre;Erbb4*$^{loxp/loxp}$ mice. Ser40 phosphorylation of tyrosine hydroxylase (TH-Ser40), tyrosine hydroxylase (TH), soluble catechol-o-methyltransferase (s-COMT), membrane-bound form of COMT (MB-COMT).

Figure 2-figure supplement 2. HPLC analysis of norepinephrine and dopamine. **A**, Representative graphs of main peaks in HPLC chromatograms. Norepinephrine; Dopamine. X-axis, retention time. **B**, Standard curves of norepinephrine (NE) and dopamine (DA).

Figure 4-figure supplement 1. There was no significant difference in body weight between control and *TH-Cre;Erbb4*$^{loxp/loxp}$ mice and no deficit of *TH-Cre;Erbb4*$^{loxp/loxp}$ mice in the prepulse inhibition experiment. **A**, No significant differences in body weight were detected between control and *TH-Cre;Erbb4*$^{loxp/loxp}$ mice. **B**, No prepulse inhibition deficit was observed in *TH-Cre;Erbb4*$^{loxp/loxp}$ mice. Unpaired two-tailed Student's t-test. Data are expressed as means ± s.e.m. *$p < 0.05$. n.s., not significant.

Figure 5-figure supplement 1. Cartogram of the colocalization of Cre/GFP-positive (Cre/GFP+) and NE neurons (TH+) in the LC 5 weeks after virus injection. Percentages of Cre/GFP+ neurons among NE neurons of the LC and of LC-NE neurons among Cre/GFP+ neurons in *Erbb4*$^{loxp/loxp}$ mice after virus injection. Three mice were studied, with three slices for each mouse.

Figure 1-Source data 1: Statistical reporting of Figure 1

Figure 2-Source data 1: Statistical reporting of Figure 2

Figure 3-Source data 1: Statistical reporting of Figure 3

Figure 4-Source data 1: Statistical reporting of Figure 4

Figure 5-Source data 1: Statistical reporting of Figure 5

Figure 6-Source data 1: Statistical reporting of Figure 6

Figure 7-Source data 1: Statistical reporting of Figure 7

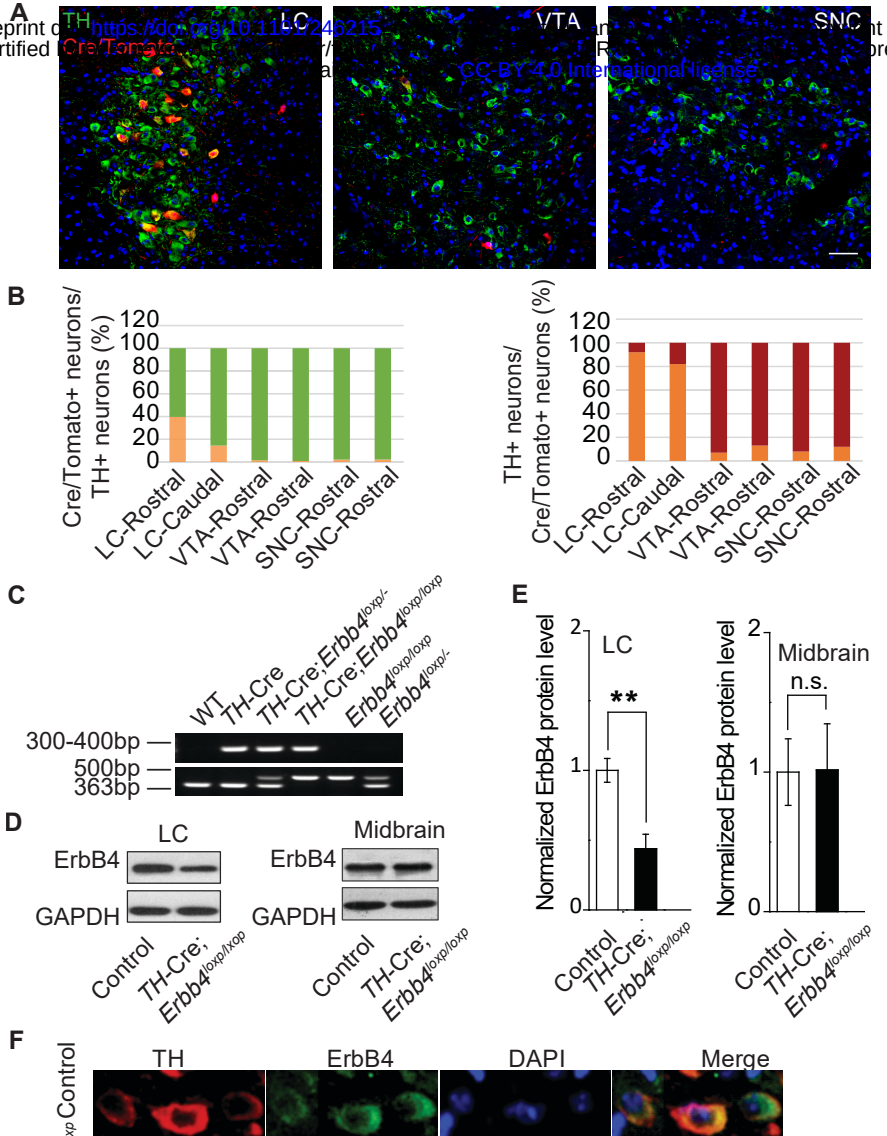

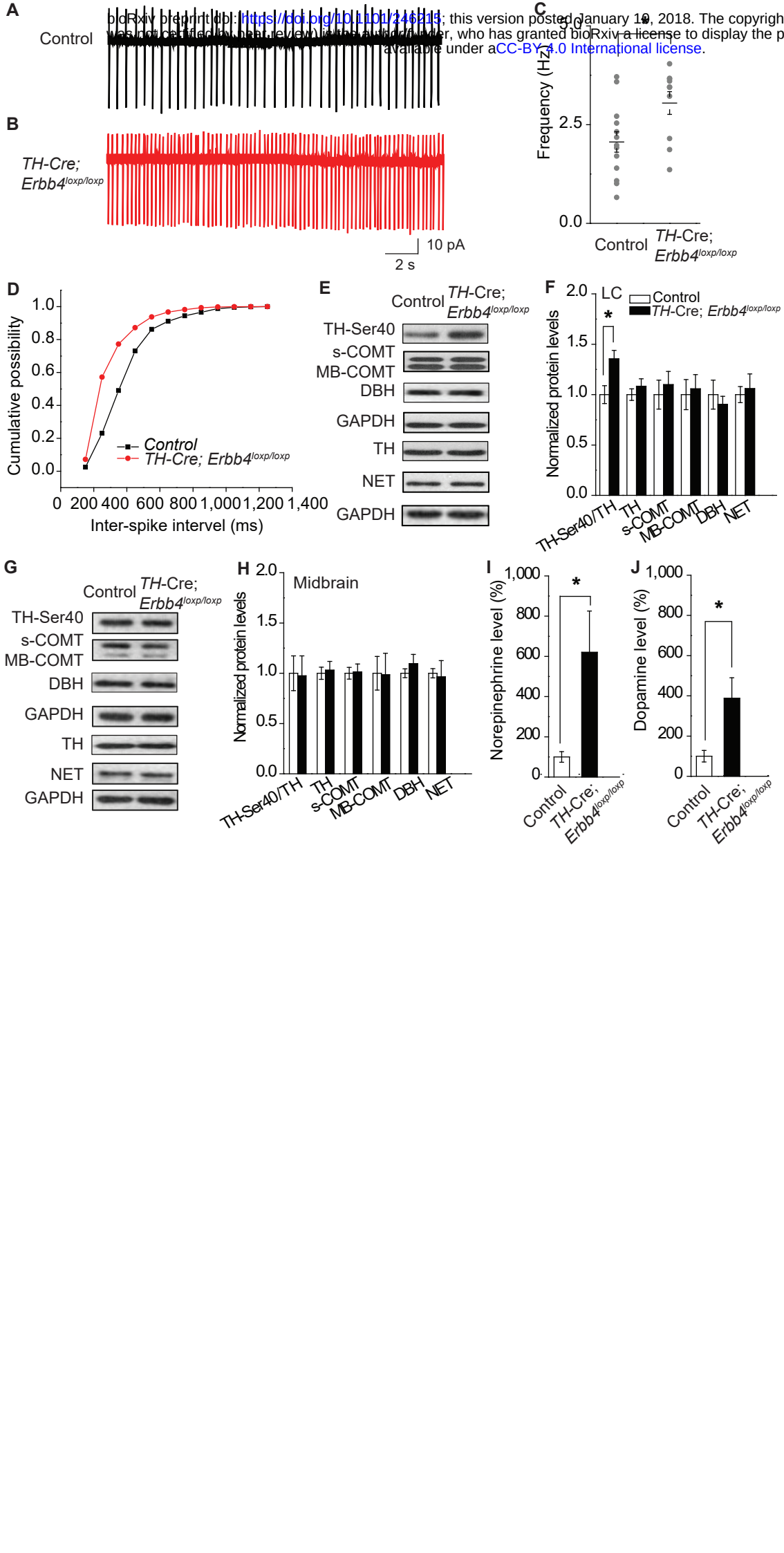

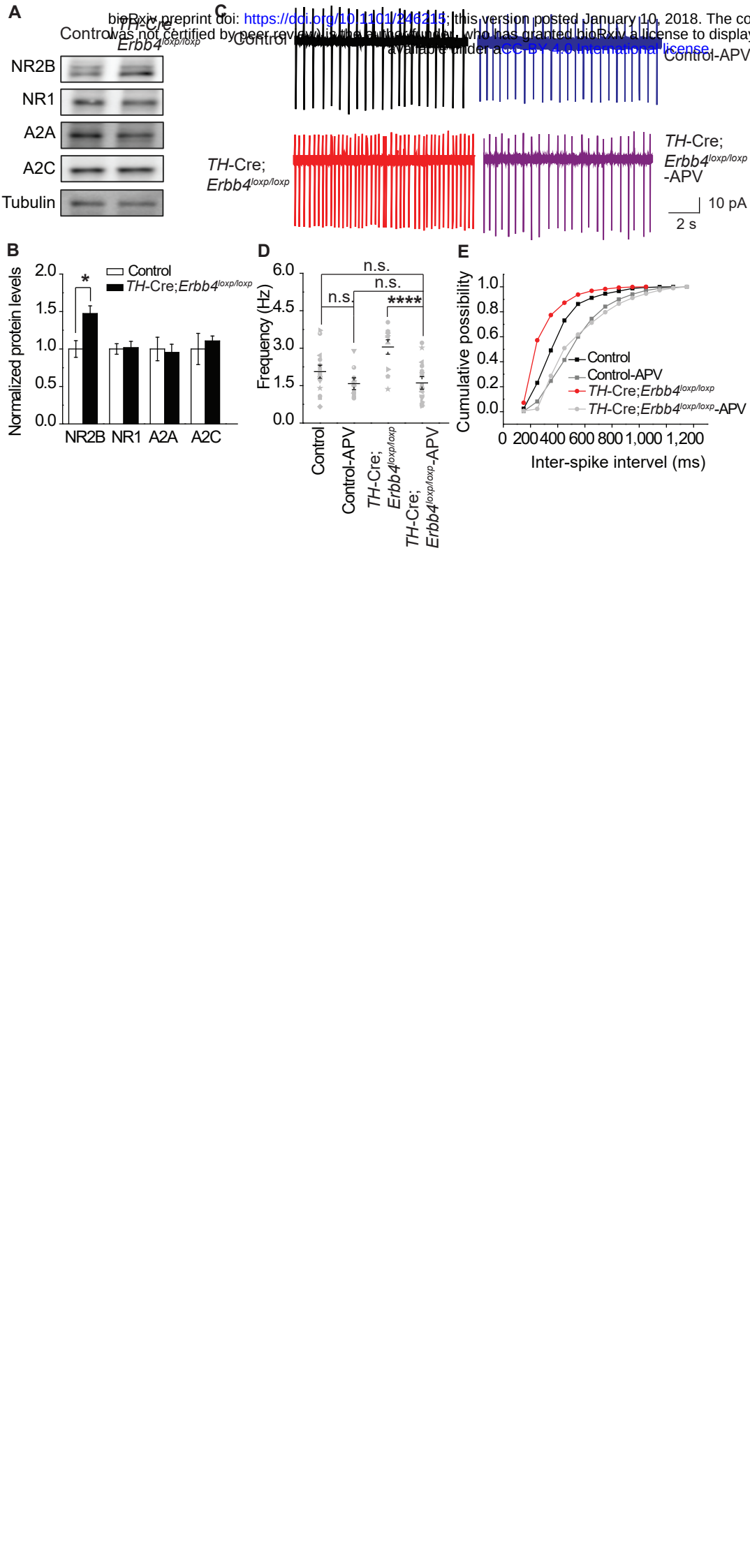

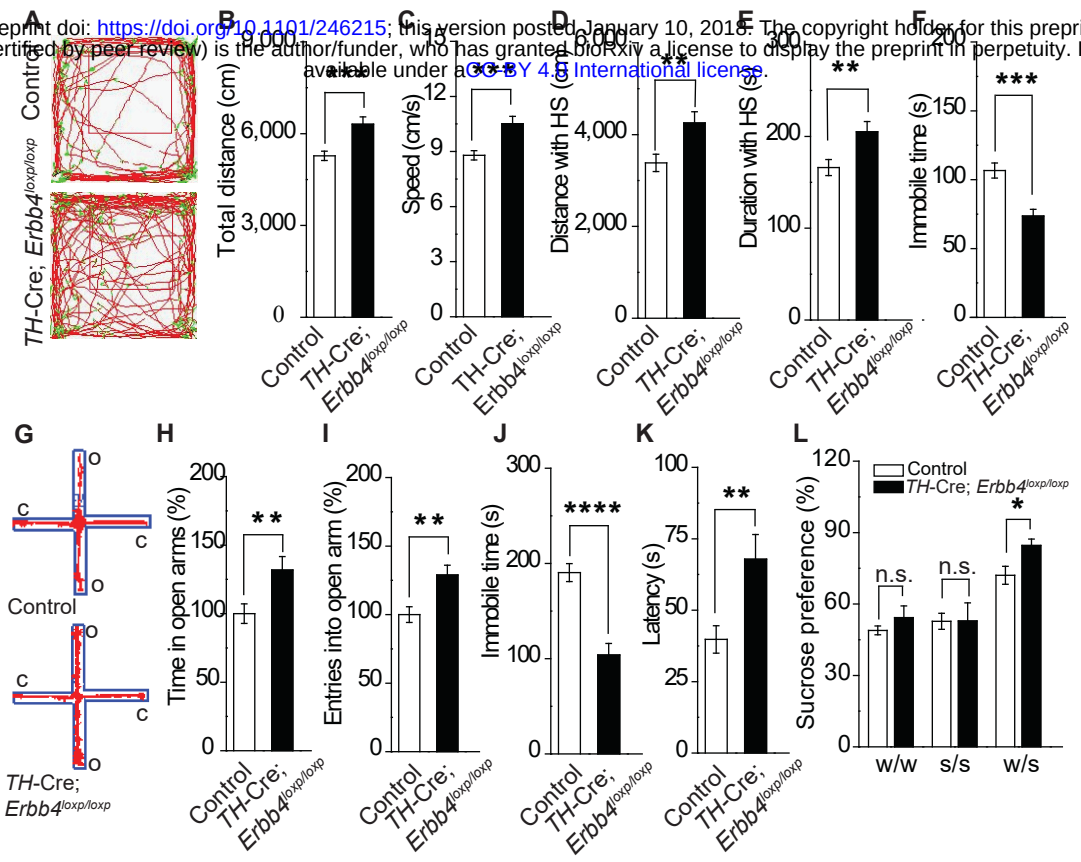

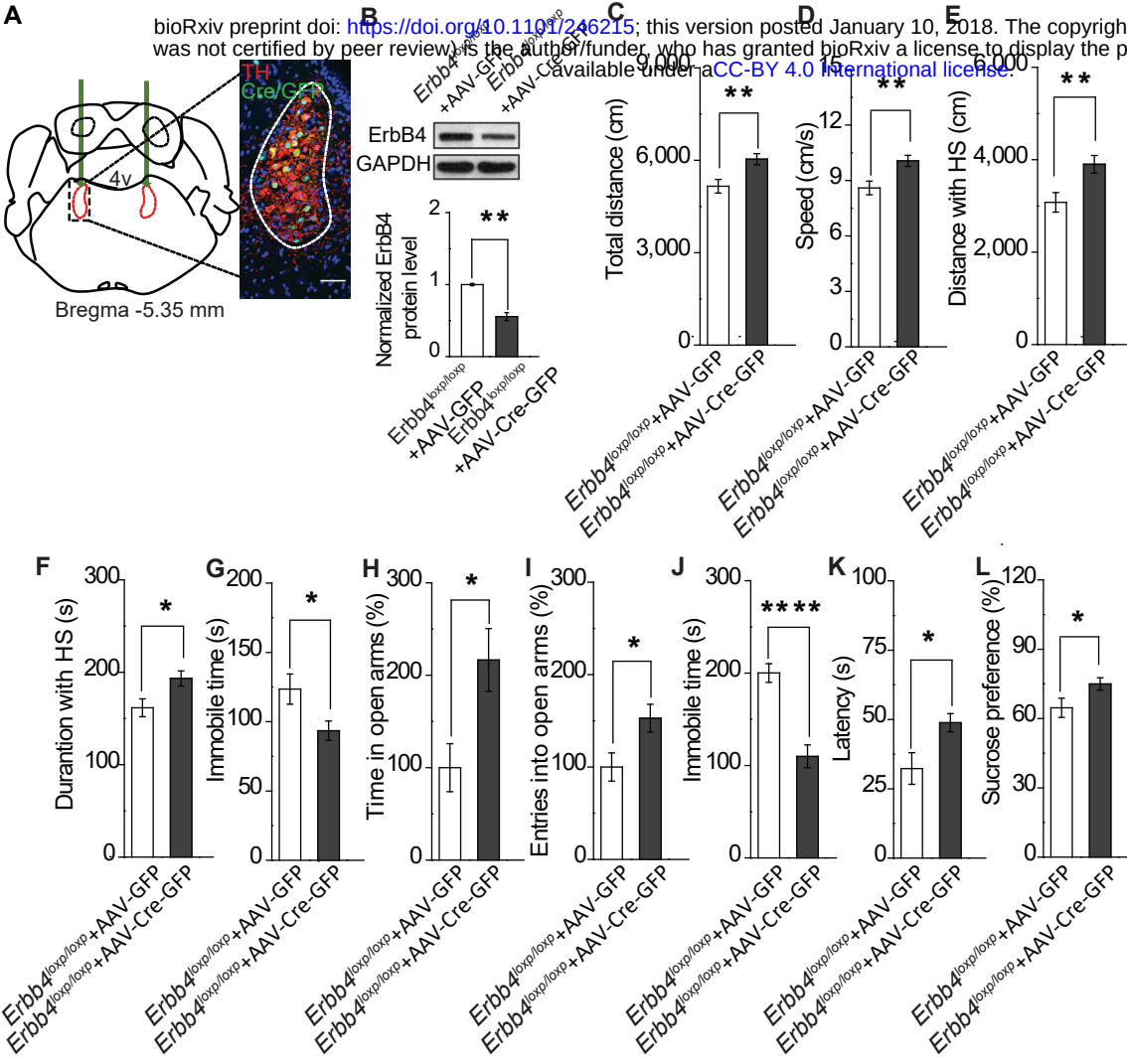

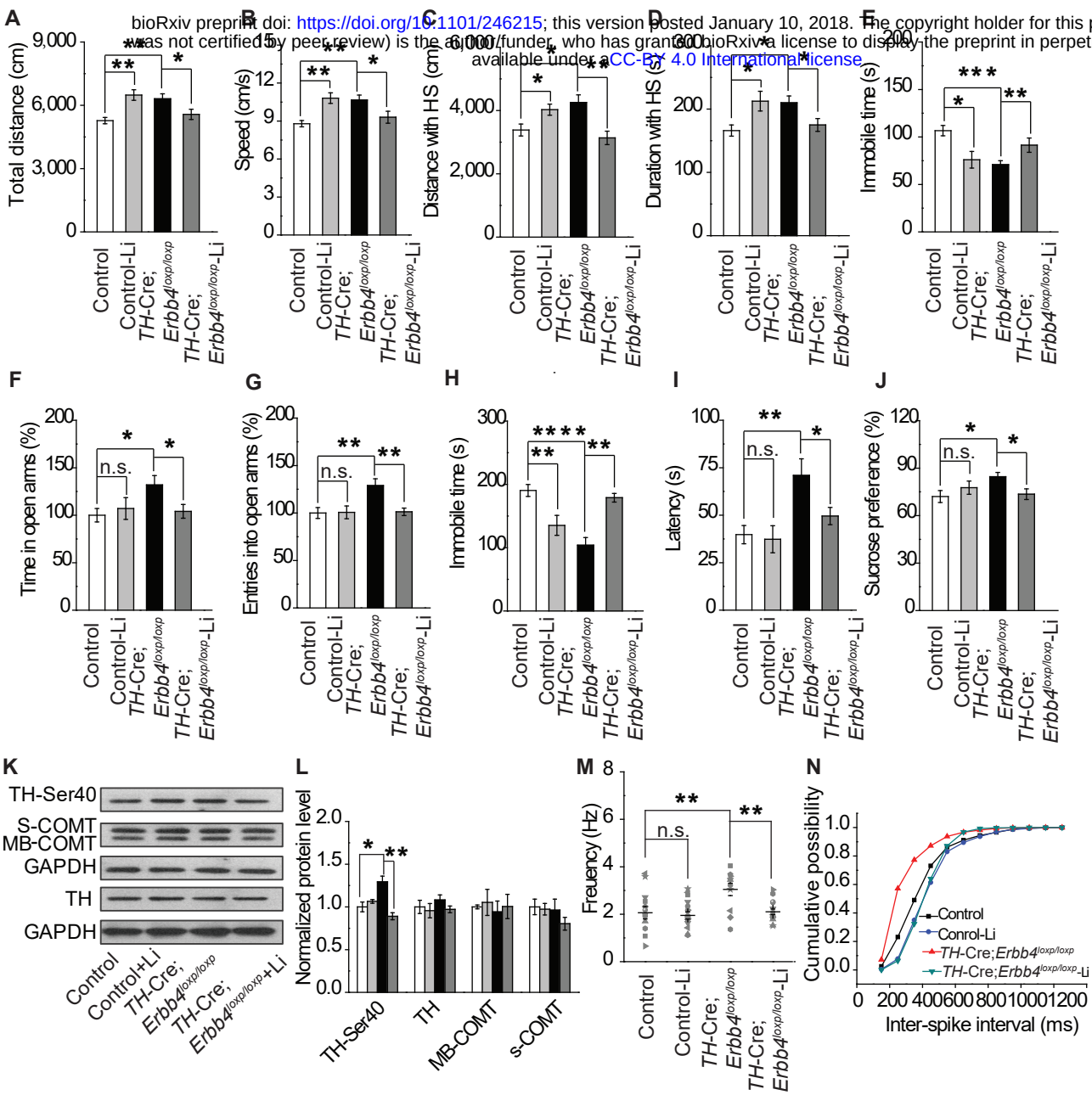

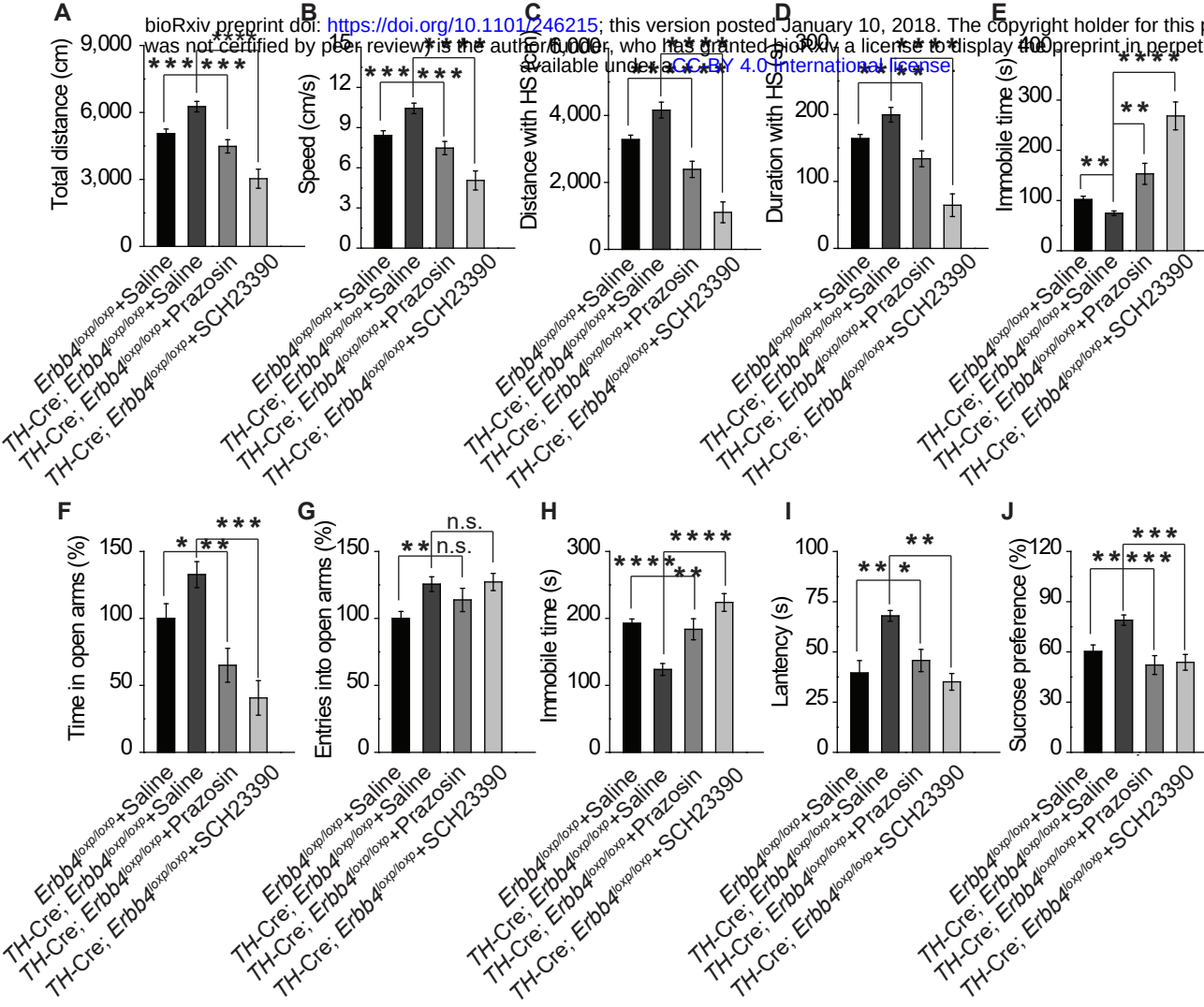

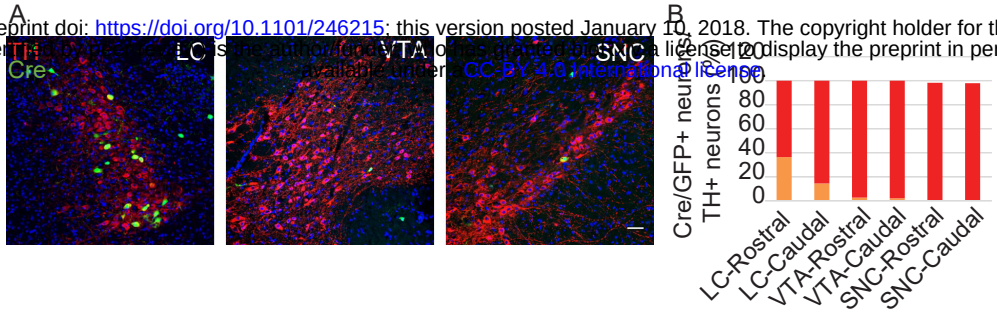

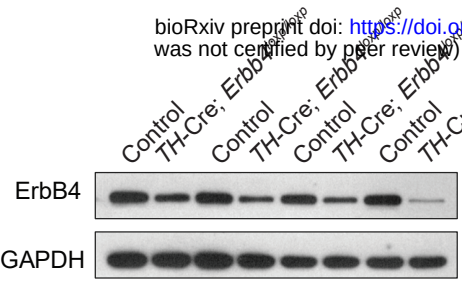

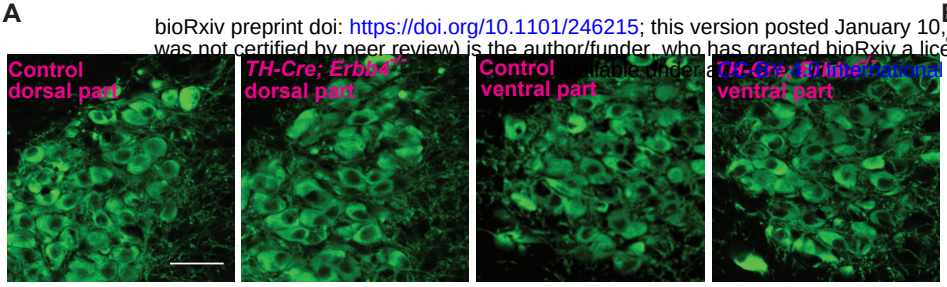

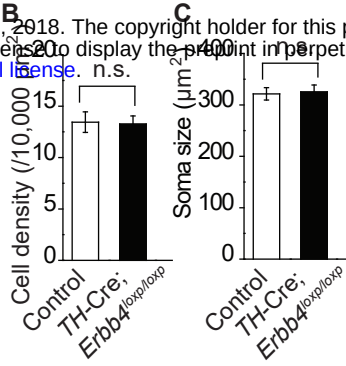

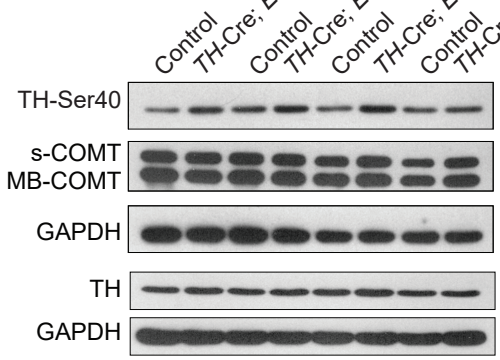

A

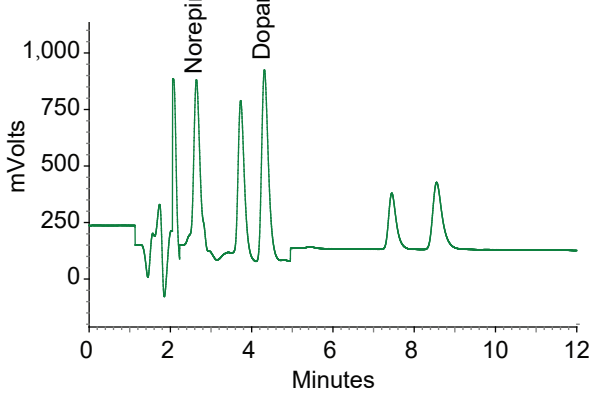

B